Investigation of the physical (rheological) properties of sewage sludge and digestate in the context of their processing in supercritical water gasification

Joanne Willemine Siccama

INVESTIGATION OF THE PHYSICAL (RHEOLOGICAL) PROPERTIES OF SEWAGE SLUDGE AND DIGESTATE IN THE CONTEXT OF THEIR PROCESSING IN SUPERCRITICAL WATER GASIFICATION

by

Joanne Willemine Siccama

in partial fulfilment of the requirements for the degree of

Master of Science

in Sustainable Energy Technology

at the Delft University of Technology,

to be defended publicly on Tuesday August 22, 2017 at 10:00 AM.

This thesis is confidential and cannot be made public until August 22, 2019.

An electronic version of this thesis is available at http://repository.tudelft.nl/.

TUDelft Delft University of Technology

Preface

In May 2010 I went to the United States, not to California or New York but to Sherwood - a village in the state of Arkansas. I stayed at a very welcoming host family located in a luxury suburb. Unfortunately, the prejudices I had were all true: energy and other resources were wasted completely. Outside temperatures went up to 40ºC, whereas inside I had to wear a sweater because I was so cold due to the air-conditioning. The house had a walkthrough shower, which literally meant water (spilled) everywhere. This experience made me realise that if people continue with this lifestyle it is no surprise that we run out of fossil fuels. In this thesis I have investigated Supercritical Water Gasification, a process to generate sustainable energy. Sustainable energy will be the (near) future, but it cannot solve the energy problem alone. As what I have learned from my stay in the USA, we have to change our consumption pattern too.

This report presents the research I carried out for my Master Thesis on the topic 'Investigation of the physical (rheological) properties of sewage sludge and digestate in the context of their processing in supercritical water gasification'.

The last six months encapsulated a wide variety of topics, commencing with a literature study, followed by laboratory work and modelling of the results. The last month was dedicated to finalising the report and preparation of my colloquium.

In this *Preface*, I would also like to take the opportunity to thank some persons who helped me during my thesis. First of all, thanks to John, Clemens and David of Gensos BV who provided a good working atmosphere with interesting discussions during lunch time. Special thanks to Clemens Schönlein, as my supervisor of the company, Clemens helped me answering questions on the process, providing useful articles and gave me feedback. Towards the end of my thesis when Clemens was no longer employed by Gensos BV he still took responsibility for being my supervisor which I really appreciate. Also, special thanks to Wiebren de Jong, as my supervisor from TU Delft and member of the thesis committee, he has seen my report many times and helped me to improve my report to this final version. Thanks to Rachel van Ooteghem for being my internship supervisor. I also want to thank Mohammed Jafar and Armand Middeldorp of the Waterlab of Civil Engineering, TU Delft for making it possible to carry out my experiments their laboratory. I also want to thank Paul Weij, process engineer of wastewater treatment plant Delfluent, who helped me collecting the samples and provided me information on sludge compositions. Furthermore, I would like to thank Sita Drost, Postdoc researcher at the fluid mechanics department, for her time to analyse and discuss my rheology results. In addition, I would like to thank Christophe Annaert and Haike Ruijters both product managers at Anton Paar Benelux, who gave me advice on the rheometer set-up and answered the questions I had. Finally, I would like to thank my boyfriend Tom Verhoek not only for his mental support, but also for the knowledge and expertise he has in the field of wastewater treatment.

I hope you will find this report both interesting and stimulating.

Joanne Siccama
Delft, August 2017

Abstract

Supercritical water gasification (SCWG) is a thermochemical conversion process in which wet biomass is converted into gaseous products as methane, carbon dioxide and hydrogen. For SCWG both the temperature and pressure of the medium are increased beyond the critical point of water (373.95ºC and 220.64 bar). The supercritical water acts as an active reactant and increases the conversion efficiency. Moreover, energy-intensive drying of the feedstock can be omitted since wet biomass can be directly introduced to the process.

An important issue related with the wet waste feed is upstream pumpability due to clogging in the pipelines. To understand this behaviour a detailed analysis of the physical parameters responsible for the pumpability of feedstock is imperative. These parameters involve particle size distribution (PSD), dry matter (DM), viscosity and homogeneity. The aim of this research was to identify the physical (rheological) properties of two feedstocks, secondary and digested sludge, and to propose a pre-treatment which could improve system performance.

To identify the physical (rheological) properties experiments have been performed in the domain of rheological methods. The PSD has been determined via laser diffraction with the *Microtrac S3500*. The rheology has been analysed with the *Anton Paar* rotational rheometer. The effects of particle size, DM content, temperature and shear rate on the shear stress and viscosity have been investigated. The acquired data provided essential information on suitable pre-treatment methods for feedstock preparation.

The results revealed that the PSD of secondary and digested sludge was below the maximum tolerated particle size for most pumping systems. The rheology data indicated shear thinning behaviour of the sludge, since viscosity decreased upon increased shear rate. Higher temperatures were also found to decrease viscosity and shear stress of the sludge.
For commercial application, the low DM concentrations of secondary sludge (4-6 wt%) and digested sludge (3-4 wt%) need to be further increased. Addition of polymers is discouraged, since it limits pumpability. Secondary sludge (< 5wt% DM) showed a logarithmic correlation between viscosity and DM. Consequently, when DM content is further increased the viscosity will become the limiting factor for pumpability.

The issue of pumpability limited by the sludge viscosity could be overcome by performing a pre-treatment with a continuously stirred tank at elevated temperatures. The viscosity is decreased when the fluid is constantly in motion and temperature will further lower the viscosity.

Nomenclature

Abbreviations

AD	Anaerobic digestion
BMC	Building Material Cell
CC	Concentric Cylinder
CHP	Combined Heat and Power
COD	Chemical Oxygen Demand
DM	Dry matter
LVER	Linear viscoelastic range
Nkj	Kjeldahl-nitrogen
OM	Organic matter
PSD	Particle Size Distribution
SCW	Supercritical water
SCWG	Supercritical water gasification
SEM	Scanning electron microscope
STOWA	Stichting Toegepast Onderzoek Waterbeheer
TS	Total solids
WWTP	Wastewater Treatment Plant

Symbols

Greek symbols

γ_{xy}, γ	Shear rate	$[s^{-1}]$
γ_A	Strain amplitude	$[\%]$
γ_c	Critical shear rate	$[s^{-1}]$
γ_L	Limiting strain	$[\%]$
γ^s	Shear strain	$[\%]$
δ_{cc}	Ratio radii of cup and bob	$[-]$
$\tan(\delta)$	Loss tangent	$[-]$
η	Viscosity	$[Pa \cdot s]$
ρ	Density	$[kg/m^3]$
σ	Standard deviation	$[-]$
τ_{xy}, τ	Shear stress	$[Pa]$
τ_0	Yield stress	$[Pa]$
ω	Angular frequency	$[rad/s]$
ω_c	Critical angular frequency	$[rad/s]$

Latin symbols

A	Area	$[m^2]$
C_{sr}	Narrow cylinder gap coefficient	$[-]$
G'	Storage modulus	$[Pa]$
G''	Loss modulus	$[Pa]$
G^*	Complex modulus	$[Pa]$
K	Power law coefficient	$[-]$
K_w	Ionic product	$[-]$
N	Sample size	$[-]$
n	Power law coefficient	$[-]$
p	Pressure	$[Pa]$
p_c	Critical pressure	$[Pa]$
Re	Reynolds number	$[-]$
R_e	Cup radius	$[m]$
R_i	Bob radius	$[m]$
T	Temperature	$[K]$
T_c	Critical temperature	$[K]$
t	Time	$[s]$
$\bar{x}$	Sample mean	$[-]$
y_{fit}	Model values	$[-]$
y	Measured values	$[-]$
V_x	Velocity	$[m/s]$
$Z_{\alpha/2}$	Confidence coefficient	$[-]$

Contents

1   Introduction

The world is still heavily relying on the consumption of fossil fuels. From the yearly 13,805 Mtoe[1] of total energy produced, 31% comes from oil, 29% from coal and 21% from natural gas (IEA, 2014). However, due to climate change and the depletion of fossil fuels the shift towards renewable energy technologies will be inevitable. As a result, research focuses on a wide variety of sustainable sources. Most of these renewables, like wind energy, solar and hydropower, are converted into electrical energy. Biomass, however, offers a broader variety of applications, it can be fed to a Combined Heat and Power (CHP) plant but it can also be used to produce liquid biofuel or biogas (Heinberg and Mander, 2009).

The market potential of energy from biomass is based on its sustainability, availability and price. These aspects vary for the type of feedstock used. This is illustrated by the three different classes in which biomass can be categorised; first-, second- and third-generation biomass. First-generation biomass uses crops which are also suitable for food or animal feed. This results in direct competition with the food crops also known as the food versus fuel discussion. The second-generation biomass covers the non-edible feedstocks like residues from the agriculture and wood industry. Finally, the third-generation biomass deals with bioenergy generated from other products like marine algae. These aquaculture based products do not compete for land use. However, third-generation biomass is not commercially available yet, since it is still in the research phase (Lee and Lavoie, 2013). In particular the second-generation biomass shows great market potential to decrease fossil fuel consumption.

An important source of second-generation biomass is wet waste, which is present in large quantities. Wet waste is mostly converted via conventional gasification and anaerobic digestion (AD), a biochemical conversion process. However, these conversion processes have some limitations. Conventional gasification requires the drying of materials until less than 30% moisture content (McKendry, 2002). Drying is an energy intensive procedure, especially since the dry matter (DM) fraction of wet waste is relatively low. AD, on the other hand, is carried out in liquid medium at mild conditions, but AD is a time-consuming operation with a relatively low conversion yield.
An alternative for these processes is supercritical water gasification (SCWG). For SCWG both the pressure and temperature of the medium are increased beyond the critical point. As a result, the present water enters the supercritical state which corresponds to a high diffusivity, a high solvability of organic compounds and a low viscosity. Furthermore, water acts as an active reactant in steam reforming and water-gas shift reactions in the supercritical region (Acelas et al., 2014). These properties lead to an efficient conversion of wet biomass into product gas. During the process no drying is required and the residence times are short (Yakaboylu et al., 2015).

The company Gensos has developed a patented technology (Harinck and Smit, 2014) to convert wet waste streams into valuable gaseous products and minerals via SCWG, producing up to 50 percent more gas as compared to AD. The technology developed by Gensos still faces some challenges in terms of making commercial application of SCWG feasible.
One of the most important issues is the diversity of wet waste feed streams which makes it difficult to predict the behaviour upon processing. As a result, an advanced understanding of relevant criteria and treatment options for wet waste feed streams is imperative.
In addition, the pumpability of the feedstock upstream at mild conditions, e.g. ambient pressure and temperature, and at high pressure and ambient temperature conditions still ambient temperature presents a challenge due to clogging in the pipelines. The following parameters play an important role for the pumpability of the sample: particle size distribution (PSD), dry matter (DM), viscosity and

---

[1] Thousand tonnes of oil equivalent on a net caloric value basis

homogeneity. In order to understand this behaviour a detailed analysis of these properties is required.

The aim of this project is to identify the physical (rheological) properties of the commercially available feedstocks and their role in the SCWG process. Until now the properties of the feedstocks have been modelled as simple Newtonian fluids (water). The characterisation of the rheological properties allows a better prediction of fluid behaviour. The second objective will involve ways to improve system performance through the investigation of different pre-treatment techniques. The objectives are summarised in one main research question and supported by a set of sub-research questions.

Main research question
What are the characteristics of different feedstocks which influence the SCWG process and which pre-treatment steps could be applied to improve system performance?

Sub-research questions
1. What are the chemical and biochemical compositions of different feedstocks?
2. What are the physical (rheological) properties of sewage sludge and digestate under different temperature and shear conditions?
3. Which pre-treatment methods are suitable for feedstock preparation?

This thesis has been focussed on the analysis of the rheological properties of two feedstocks in particular; secondary sludge and digested sludge. Both feedstocks are produced during wastewater treatment and were collected at the wastewater treatment plant (WWTP) Delfluent in Harnaschpolder. The samples have been analysed via experiments in the domain of rheological methods. These experiments gave information on PSD and DM content of the feedstocks, important parameters to describe pumpability. In addition, the effects of particle size, DM content, temperature and shear rate on the shear stress and viscosity have been investigated to define if they could improve system performance. The results obtained from the temperature effect have been used to develop a model to describe the shear stress as a function of temperature. This model is a convenient tool to make a prediction of the temperature influence. Finally, the long-term stability of the sample has been defined to predict if phase separation would occur upon storage, making the sample inhomogeneous which increases the likelihood of clogging.

2 Literature study

2.1 Supercritical water state

The supercritical water (SCW) state is described as a dense fluid state in which one cannot distinguish liquid and vapour phase anymore. This can also be observed from the phase diagram in Figure 2.1, beyond the critical point there is no clear distinction between liquid and gas.

The following critical parameters for temperature and pressure are obtained from the *Industrial Formulation 1997* released by the *International Association for the Properties of Water and Steam* (IAPWS, 2007).

$$T_c = 647.096 \text{ K } (373.95°C)$$

$$p_c = 22.064 \text{ MPa } (220.64 \text{ bar})$$

The properties of SCW differ from normal liquid or steam at atmospheric pressure.

The density at the critical point is around 300 kg m^{-3} whereas density of liquid water at ambient conditions is 1000 kg m^{-3}. Also, the ionic product represented via $K_w = [H^+]*[OH^-]$ is increased with a factor 1000 around the critical point, since it goes from 10^{-14} to $\sim 10^{-11}$.

In the vicinity of the critical point where the ion product is relatively high ($\sim 10^{-11}$), the $[H^+]$ concentration is about 30 times higher than at ambient conditions, offering increased opportunities for acid-catalysed reactions (Kersten and de Jong, 2014) and resulting in pH decrease by 3 units (Brunner, 2009).
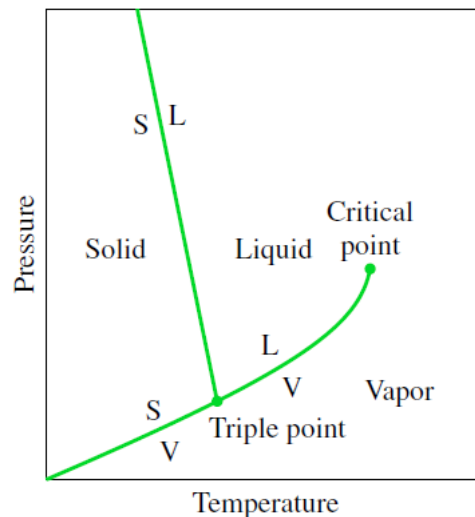

Figure 2.1: Phase diagram of water (Moran and Shapiro, 2006)

Liquid water at ambient conditions is a polar solvent with a dielectric constant of 80. As a result, it has a relatively low solubility for nonpolar organic compounds like benzene and a high solubility for inorganic salts. Around the critical point, however, the dielectric constant is lowered to 5, which makes the solvent nonpolar resulting in a high solubility for nonpolar organic compounds. In addition gases like carbon dioxide, methane, nitrogen and oxygen are completely miscible in SCW (Kersten and de Jong, 2014). The solubility of inorganic salts, on the other hand, drastically decreases which offers several possibilities for separation and recovery of for example phosphorus. Phosphorus is an important constituent for fertilizers used in agriculture. Almost all phosphorus currently used is derived from phosphate rock. However, both the availability and quality of the mineral phosphate resources are decreasing, leading to an increase of the phosphate rock price and alternative resources for phosphate fertilizers production will become more important (Acelas et al., 2014).

2.2   Supercritical water gasification

SCWG is a thermochemical conversion process in which wet biomass is converted into gaseous products as methane, carbon dioxide and hydrogen at supercritical conditions. An advantage of SCWG over conventional gasification is that wet biomass can be directly introduced to the process , thus energy-intensive drying of the feedstock can be omitted (Yakaboylu et al., 2015).

In Figure 2.2 the process flow diagram of SCWG system developed by Gensos is represented. All unit operations will be explained step-by-step. In Figure 2.3, the simplified process flow diagram of the SCWG is represented including information on temperature and pressure. This scheme involves all reaction steps, the gas separation and upgrading at the end of the process.
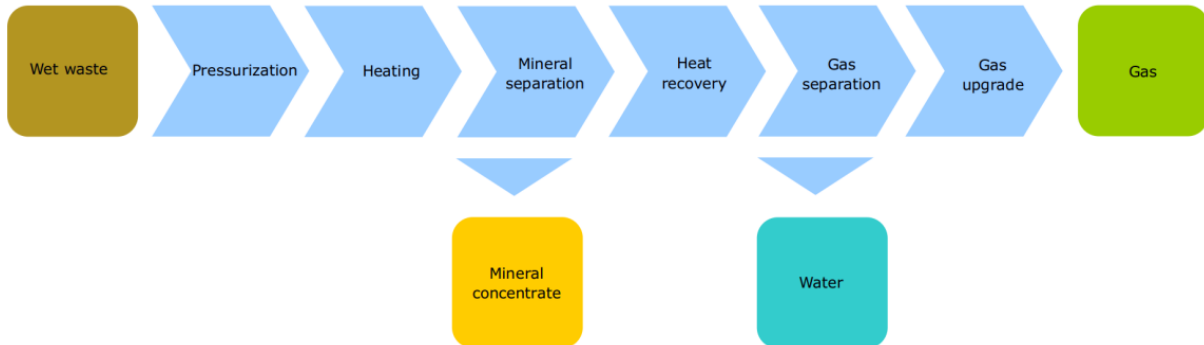

Figure 2.2: Process flow diagram of the supercritical water gasification system developed by Gensos (Gensos, 2015)

Wet waste – The origin of the feedstock for SCWG may vary. Suitable options are sewage sludge, dredging sludge, algae, animal manures and residues from a fermentation facility (Harinck and Smit, 2014). All feedstocks are characterised by their high moisture content. Gensos has experimented with wet waste up to 10 wt% dry matter (DM) content. Other papers showed higher values. The *Stichting Toegepast Onderzoek Waterbeheer* (STOWA) had successful experiments with sewage sludge up to 17.4 wt% DM (Korving, 2016). Zhai *et al.* experimented with sludge concentrations between 5 and 25 wt% (Zhai et al., 2013).

In their patent Gensos stated that the wet biomass as fed to the gasification process comprises DM of at least 5 wt%, relative to the total weight of wet biomass. The DM content in the normal practice is at most 60 wt% on the same basis (Harinck and Smit, 2014).

The DM concentration of the feedstock is an important parameter since it has significant influence on the economic feasibility. A higher sludge concentration would lead to a smaller installation and an enhanced heat management. On the other hand, a high concentration increases the chance of clogging. In addition, a higher concentration would lead to a lower conversion yield of biomass derived product gas (Korving, 2016).

Pressurization – In the first stage of the process the wet biomass will be pressurized with a high-pressure pump to approximately 240 bar, which exceeds the supercritical pressure of 221 bar.

The pressurization can be done via two different pump types. The first option is a linear displacement pump (piston-in-cylinder), which pressurizes the feedstock through volume reduction of the chamber by exerting a high force on the piston in the opposite axial direction (Harinck and Smit, 2014). The other pump is the diaphragm pump produced by manufacturers as LEWA and Feluwa. This pump is often used in the mining industry since it is well suited for pumping viscous materials and materials with a high solid content (Hicks, 1988).

For the optimisation of the process a possible pre-treatment step could be implemented before the pressurization. Potential pre-treatment steps will be further investigated in this thesis report.

Heating – Before entering the reactor the wet biomass will be heated up to reach sub-but near-critical conditions, defined as water temperatures above the boiling and below the critical point (Möller et al., 2011). From the output of the preheater in Figure 2.3 it can be observed that

temperatures of 370ºC will be achieved, which is near to the supercritical temperature of 374ºC. Inside the reactor the temperature will be further increased, which guarantees that supercritical conditions will be reached.

It needs to be noted that the reactions take place in all heat exchangers in the SCWG process, which means that not only a single reactor exists. In the schematic overview these heat exchangers are indicated as *preheater*, *reactor* and *superheater*. Especially in the superheater strict safety measures are required for the material, since the steel needs to withstand not only very high pressures, but also temperatures in the range of 600-650ºC. At these conditions a residence time of 30, 60 or 120 seconds is required to enhance the conversion yield.

Mineral separation – Under supercritical conditions minerals will precipitate. The mineral separation is a unit operation which has not been implemented yet in the pilot plant of Gensos. The focus until now has been on the generation of biogas and gas cleaning over the mineral separation. Based on different reasons the mineral separator can be placed either before or after the *superheater*. When the minerals separator is located before the superheater corrosion and clogging caused by the salts is prevented. Placing the separator after the superheater, on the other hand, prevents the fact that unreacted organic particles will be removed before the gasification which would increase the conversion yield of the process (Korving, 2016).

The process flow diagram in Figure 2.3 shows that the minerals will be most likely separated via an additional separation unit when the product leaves the *reactor* at a temperature of 500ºC, but before it enters the *superheater*. The minerals could be separated by a cyclone.

Heat recovery – In order for the process to be energetically efficient, outlet flows at high temperature can be returned to the heat exchanger to preheat the incoming flow. This is also shown in Figure 2.3 where recycle streams are used to heat up the influent of the preheater and reactor. It is important to notice that heat cannot be completely recovered. The maximum heat recovery of a process can be determined using a pinch analysis. The heat transfer cannot be 100% since there has to be a minimum energy difference and therefore a temperature difference. Aspects such as resistance of heat transfer layers and losses to the environment are taken into account in this temperature difference (Boom, 2015).

From Figure 2.3 it can be observed that the *superheater* is not heated with the process streams, but by a flue gas burner. For the superheater the driving force plays an important role.

The heat exchanger of the reactor has a significant temperature difference when the start temperatures are 370ºC and 600ºC. This enhances a good heat transfer, especially if the heat streams flow counter-current direction. In this manner a higher rate of heat transfer per unit area would be obtained compared to a co-current heat exchanger (Boom, 2015).

Gas separation – In this step the gas and liquid will be separated. At first the fluid gasification product will be depressurized after which the product can be flashed which leads to a syngas fraction and a contaminated water fraction. It has been found that flashing at a higher pressure leads to less CO_2 and H_2S in the syngas (Korving, 2016).

Gas upgrade – The most important compounds of the syngas are CH_4, CO_2 and H_2, of which their ratio is based on the DM content of the feedstock, the temperature and pressure conditions of the SCWG process (Kersten and de Jong, 2014). However, this obtained syngas is still strongly contaminated with products as ammonia, tar compounds and CO (Rulkens and Wentink, 2013). Therefore, it needs to be purified, for example with the use of membrane separation.
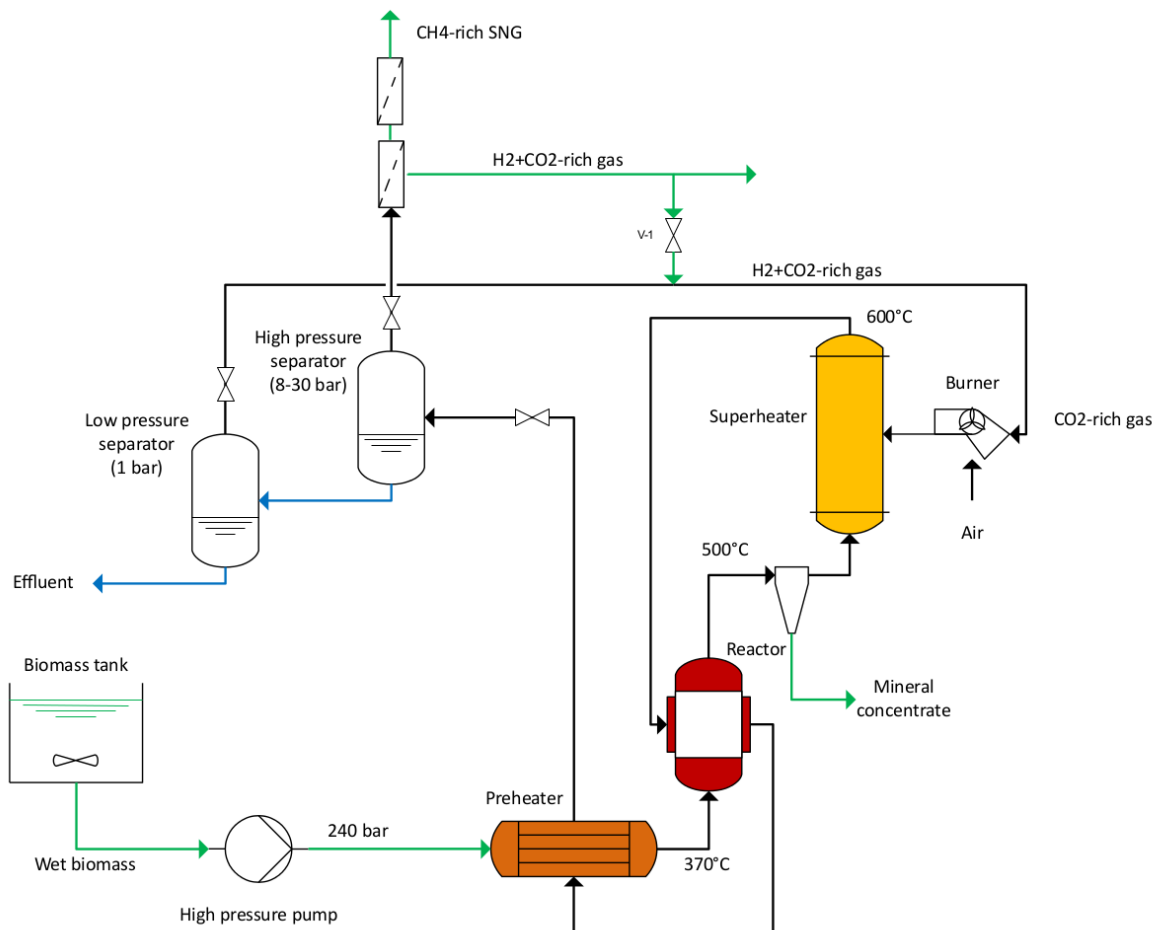
Figure 2.3: Simplified process flow diagram of the supercritical water gasification system developed by Gensos (B. V. Gensos, 2017)

2.3 Sludge treatment

Sewage sludge is a suitable feedstock for SCWG due to its large fraction of organic matter (OM), 50-80% on dry basis, and high availability. In this section a short introduction will be given on the composition and processing techniques of sewage sludge.

Sludge is the collective term to describe settle-able compounds which can be removed upon wastewater treatment. Sludge can be divided into primary and secondary sludge, of which the names relate to the part of the process where the products are formed.

The sludge treatment process will be explained step-by-step.
The influent directly comes from the sewer system and consists mostly of wastewater from households, but may also contain industrial wastewater discharges. In addition, the drainage of rainwater will also contribute to the total wastewater flow and strongly affect the capacity of a Wastewater Treatment Plant (WWTP).
The influent can go either directly to the pre-sedimentation tank or optional a sieve for large debris removal. The sieved bulky waste residue is then moved to containers, pressed and incinerated. The filtrate is directed to the pre-sedimentation tank where the primary sludge is formed. In this open-air tank 40-60 wt% of the particles will be removed within 4-6 hours. The fats and oils start floating on top and the heavy particles will sink to the bottom of the tank to form the primary sludge. A skimmer is used to separate the fats and oils.

Secondary sludge (activated sludge) is all the sludge settled in the secondary settling tanks. The sludge is formed during the biological treatment of wastewater. Aeration of wastewater increases the oxygen concentration, which in combination with the high nitrogen, phosphorus and organics concentration causes microorganisms to grow. The microorganisms grow in flocs which when settled in the secondary settling tanks causes flocculation of particles. Part of the sludge settled is recycled, the microorganism in this sludge continue to treat the wastewater. The excess sludge has to be disposed (Sanitary-Engineering, 2016). The excess secondary sludge will be sent to a digester, where it is mixed with primary sludge. The ratio between the two is roughly 50/50, but depends on the available quantities of each stream.

In the digester biogas is formed and will go to a CHP plant to produce heat and electricity. The produced heat is used to heat the inlet streams of the digester to reach the operation temperature of around 35ºC. The electricity can be used by the WWTP itself or can be fed into the grid. The residence time of the sludge in the digester is approximately 20 days. More information about the digestion process itself will be explained in section 2.4.12.4. The digested sludge at the outlet contains around 3-4 wt% DM and will be centrifuged to remove water. In some cases polymers will be added to improve dewatering and magnesium for struvite formation. The removed water will be transported to the beginning of the whole treatment process (influent). The resulting dewatered digestate is a solid clay-like product with a DM content of around 22 wt%. The dewatered digestate is normally directed to incineration plants by trucks or used as dried granules for the cement industry.

A process scheme of the sludge treatment has been made and is represented in Figure 2.4.
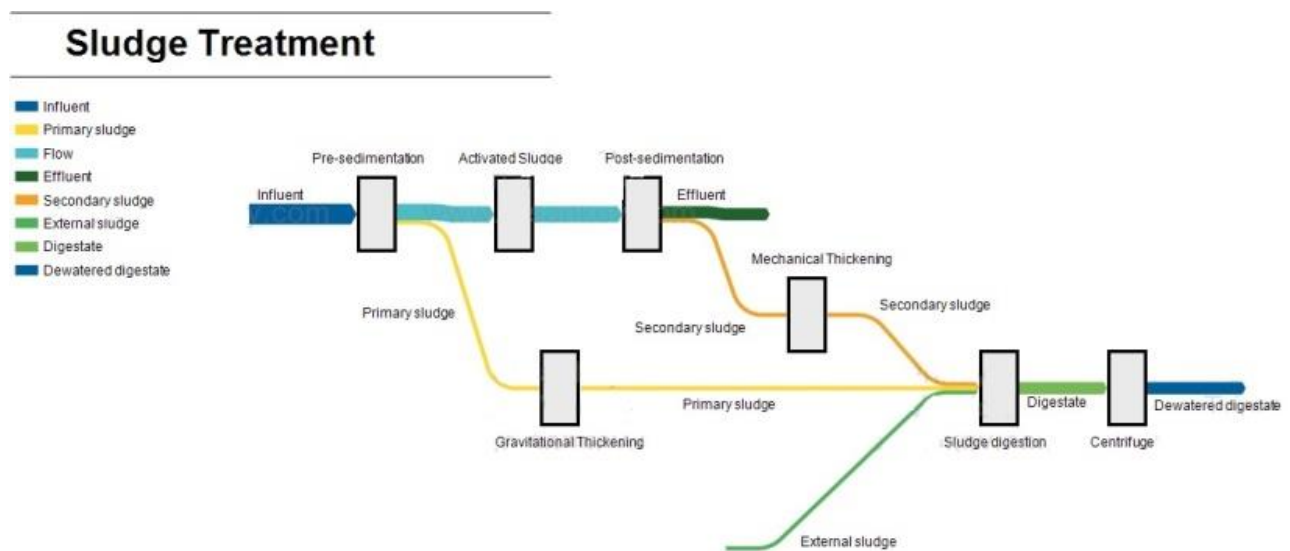

Figure 2.4: Process flow scheme of sludge treatment

2.4   Anaerobic digestion

The residual product of AD, digestate, is also indicated as biogas effluent, biogas residues or biogas slurry (digestion of animal manures). Based on the exact feedstock composition about 20–95 wt% of the OM from the feedstock is biologically degraded (Möller and Müller, 2012). The feedstocks used for AD are very diverse. Sewage sludge, manure and biowaste are examples of products which are commonly used.

2.4.1   Sewage sludge digestion

As indicated in section 2.3, the sludge digestion is a standard procedure at the WWTP. There are several reasons for the implementation of sludge digestion:
1. It improves the dewatering capacity of the excess sludge. Fresh sludge has proven to absorb more water than digested sludge.

2. The organic fraction of the sludge is reduced, which consequently decreases the sludge volume.
3. The sludge is fully stabilised. This prevents further degradation and the formation of odours compounds.
4. The OM is converted into an energy-rich biogas.
5. It improves the hygienic quality of the sludge.

The composition of the primary sludge significantly differs from the secondary/biological sludge. Primary sludge consists of more easily digestible carbohydrates and fats, whereas the biological sludge contains more complex carbohydrates, proteins and long chain hydrocarbons. These properties have an impact on the anaerobic digestibility. The primary sludge digestion usually leads to high volatile solids destruction. The components of the secondary sludge present a challenge, and should be broken down to more fundamental or soluble components in order to become better degradable by anaerobic digestion (Gary et al., 2007).

The biogas yield depends on the exact sludge composition, but on average this is about 1000 L/kg of destructed organic material (van Lier and de Kreuk, 2016-2017). The composition consists of a mixture of 60-65% methane and 35-40% carbon dioxide, which has a caloric value of 24 MJ/m^3 (van Lier and de Kreuk, 2016-2017).

Sludge digestion reduces the sludge OM by about 50%, in addition the dewaterability of the sludge is improved (Sanitary-Engineering, 2016). Sludge disposal is expensive for WWTPs with costs of around 70 euros for 1 m^3 (Ringoot and Reitsma, 2014).

Whereas for other products the digestate is often used as a fertilizer, for sludge digestate this is not the case. This is due to legislation, since the heavy metal content of the product is too high (van Lier and de Kreuk, 2016-2017) and although the hygienic quality has improved the product is not free of germs (Sanitary-Engineering, 2016).

2.4.2 Biowaste digestion

Biowaste digestate is another interesting feedstock for SCWG. This feedstock has been used for experiments in the pilot plant of Gensos. An issue with this feedstock is the large quantity of sand present in the sample. In the trial experiments this has caused clogging of the pipelines. For SCWG the inorganic sand fraction is preferably removed, since it cannot be converted to biogas. The sand could be removed with the use of a decanter, also represented in the mass balance of the biowaste digestion process from Figure 2.5. A disadvantage of the decanter, however, is that not only sand will be removed but also part of the organic fraction.
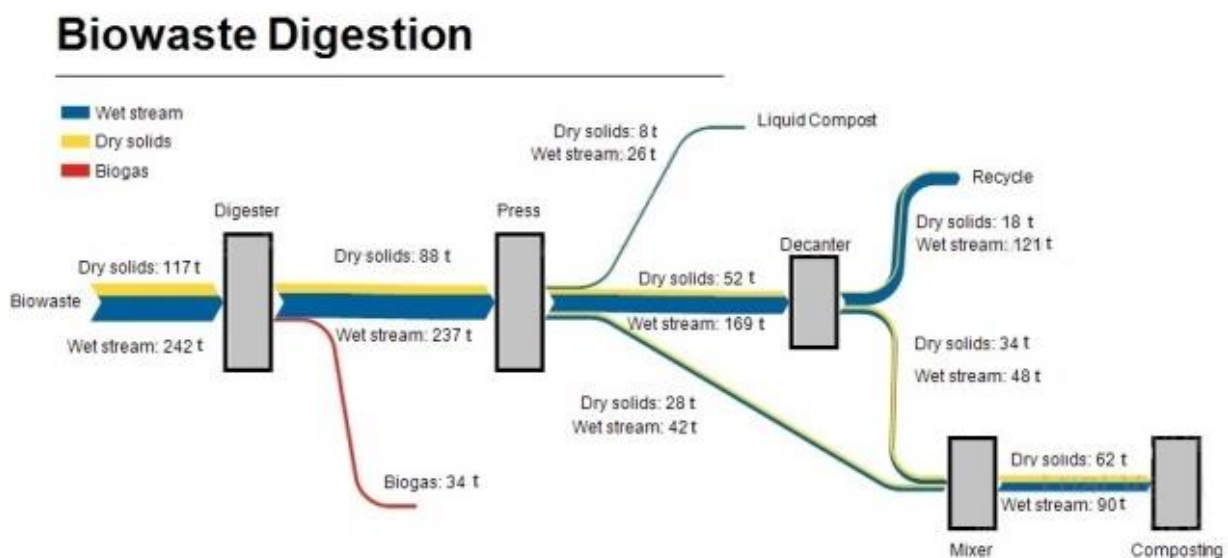

Figure 2.5: Process flow scheme of biowaste digestion, the quantities are based on a fermenter in Middenmeer and represented in tonnes per day (Froeling, 2012c)

From the mass balance it can be observed that without SCWG about 30 wt% of the incoming dry solids stream is converted to biogas. The use of SCWG could lead to higher conversion yields, since (nearly) all organics compounds can be converted to biogas. The exact conversion yield is based on the type of process flow used for SCWG. When the pressed water with OM of 37.5% (Froeling, 2012a) is used for SCWG conversion yields could go up to ~46 wt% of incoming dry solids. When the pressed water first goes to the decanter, the filtered outgoing flow (centrate) has an increased OM of 64% (Froeling, 2012b) due to the sand removal. However, the dry solids content is also reduced. When the centrate is used for SCWG the conversion yield could reach a maximum of ~39 wt% of incoming dry solids, lower than for pressed water but with a reduced chance of clogging upon SCWG.

2.5   Fluid properties

Fluids can be characterised by viscosity and shear stress as a function of shear rate. Here, a distinction is made between Newtonian fluids which obey Newton's Law and non-Newtonian fluids which do not (Akker, 2014).

Newton's Law:

$$\tau_{xy} = \eta \frac{d}{d\gamma} V_x = \eta \dot{\gamma}_{xy} \tag{2.1}$$

Here τ_{xy} presents the shear stress and is a function of shear rate $\dot{y}_{xy}$ and (shear) viscosity η.

Fluids are considered Newtonian if viscosity is independent of shear rate and there is a linear correlation between shear stress and shear rate. An example of a Newtonian fluid is pure water. Fluids are considered non-Newtonian if the viscosity changes upon different shear rates. Fluids can be classified as pseudoplastic (shear thinning) if viscosity is inversely dependent on shear rate or dilate (shear thickening) if viscosity increases with shear rate. Two other forms of nonlinear behaviour are Bingham plastic and Bingham pseudoplastic. In both cases the material only exhibits flow above a certain stress. Below this stress the material behaves solid-like. In Figure 2.6 the relationship between shear stress and shear rate is shown for the previously discussed fluids.
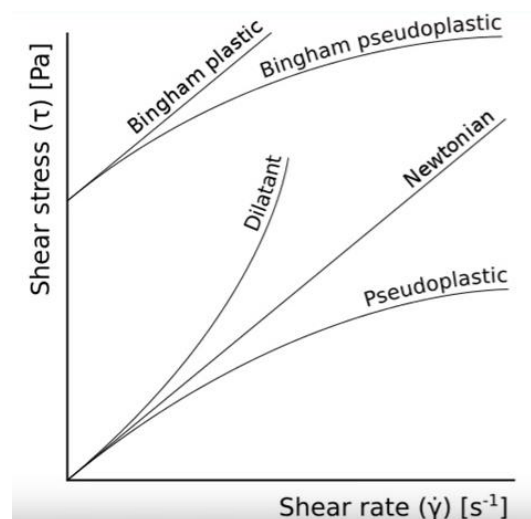

Figure 2.6: Shear stress as a function of shear rate for several kinds of fluids (RheoSense, 2015)

Material is also characterised by the degree of solid-like versus (viscous) liquid like behaviour. This behaviour is analysed via relationship between deformation and stress response. In general, small and

fast deformations have an elastic response and the material behaves like a solid. For large and slow deformations material behaves as a viscous liquid. Most materials behave in between these two extremes, also defined as viscoelastic behaviour (Venema and Sagis, 2012).

The viscoelastic behaviour is defined according to G' and G''. Here, G' describes the *storage modulus*, a measure for the amount of energy that is reversibly stored in the material during deformation. G'' describes the *loss modulus*, a measure for the energy lost during deformation as a result of viscous friction.

Together the storage modulus and loss modulus form the *complex modulus*, represented via the following equation:

$$|G^*| = \sqrt{G'^2 + G''^2}$$
(2.2)

This leads to:

$$\frac{G''}{G'} = \frac{\sin \delta}{\cos \delta} = \tan \delta$$
(2.3)

This ratio indicates how viscous or elastic the material is, referred to as *loss tangent*.
When $\tan \delta < 1$ the material is considered elastic/gel like and when $\tan \delta > 1$ it is viscous.

In many viscoelastic materials the parameters G' and G'' are not constant in time. This can be observed in thixotropic fluids where a weak solid-like structure in the material is gradually destroyed by the applied shear. These fluids exhibit time-dependent behaviour; they show a weak reversible self-association mechanism that takes a measurable amount of time to re-associate (Venema and Sagis, 2012). This mechanism can be defined through the performance of a hysteresis test; by first increasing the shear rate to a certain value followed by decreasing the shear rate and measure the shear stress. For thixotropic fluids, when the shear rate is slowed, the viscosity does not follow the same path on structure breakdown and recovery. In other words, the stress path is lagging and a hysteresis loop is formed. The area between the two curves indicates the hysteresis loop area and represents the energy consumed in structure breakdown (Franck, 2017).

The analysis of the viscoelastic parameters has been tested via an oscillatory shear experiment. More information on this experiment can be found in subsection 3.3.5.

2.6 Hydrocyclone

In order to enhance pumpability of the biomass it could be advantageous to pre-treat the biomass with a hydrocyclone for sand removal.

This technique is already applied in some WWTP. There are several reasons why sand and grit should be removed from wastewater:
- To extend the lifespan of the mechanical components, especially pumps.
- To prevent sand and grit from getting into the pipelines and machinery, valves, tubes, sealing this may cause blockages.
- To avoid depositing a sand layer at the bottom of the digestion tank, the presence of which would minimize the effective volume and hence the efficiency of the tank.
The mentioned reasons also apply for SCWG. In addition, if only the inorganic fraction of sand and grit could be removed the organic fraction will increase which is also beneficial for the conversion yield.

In the WWTP the hydrocyclone technique is mainly used for concentrated sludge flows. The hydrocyclone is a cylindrical construction with a conically tapering base. The supply of sludge mixture flows along the circumference described as a tangential supply. The separation of the heavier particles

is based on the centrifugal force caused by a gauge pressure of 500-1000 kPa. The spiral flow pushes the particles to the cone wall where they slide down to the bottom after which they can be removed. The lighter particles meet at the centre of the hydrocyclone and together with the water will flow upwards to the outlet at the top of the cyclone (Sanitary-Engineering, 2016).

In Figure 2.7 a schematic overview of a hydrocyclone is represented. On the left side the sand-sludge mixture enters the hydrocyclone after which the sludge leaves the cyclone on top and the sand is collected at the bottom.
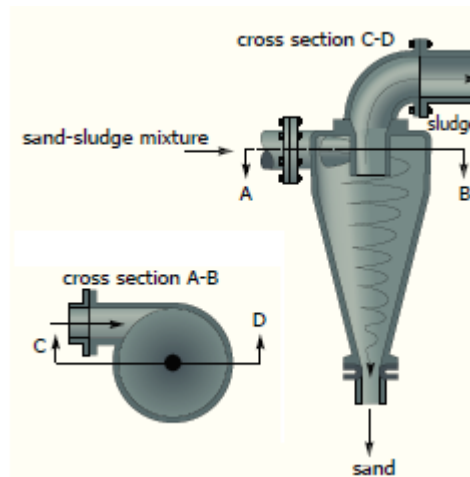

Figure 2.7: Schematic overview of a hydrocyclone (Sanitary-Engineering, 2016)

3 Materials and methods

To study the research objective and find answers to the research questions an experimental setup is designed. The experimental setup is discussed per experiment and not per research question, since some questions involved multiple experiments. In this chapter the experimental variables which are examined and the materials being used are described.

3.1 Determine feedstock composition

The first research question focusses on the chemical and biochemical composition of different feedstocks. This is an important aspect in understanding the rheological behaviour of the feedstocks. The analysis of the composition has been carried out via a literature study. Since sufficient data was available in papers, it was not necessary to carry out experiments in lab. However, there is always a strong variation in biomass samples of the same feedstock. Thus, the values found should be taken as an estimate of the composition of the samples used for the SCWG.

Not all data has been collected from papers. Gensos already tested the composition of two different biowaste digestate samples. This standard analysis has been carried out by an external party and this data has been provided by Gensos. The biowaste digestate samples found their origin in Middenmeer, Noord-Holland and in Zwolle. These samples have only been analysed for chemical composition, the biochemical composition is therefore retrieved from the literature.

The chemical composition involves total solids (TS), also defined as DM content. The OM fraction indicates the conversion potential to biogas and is expressed as a percentage of the DM. The Chemical Oxygen Demand (COD) indirectly defines the organic compounds fraction via complete chemical oxidation. The COD test is limited though since it cannot distinguish biodegradable from biologically inert OM (Kosseva, 2013). The nitrogen content can be defined via Kjeldahl, also referred to as Kjeldahl-nitrogen (Nkj). It determines the content of total organically bound nitrogen found in proteins and ammonium ions (Sanitary-Engineering, 2016).

The biochemical composition describes the DM content via carbohydrates, proteins and fats. Carbohydrates are subdivided in fibres like cellulose, hemicellulose and lignin. The biochemical composition is an important tool to describe the behaviour of rheology. For example, heating may cause denaturation of proteins. A high protein concentration could significantly impact the rheological behaviour. To define the biochemical composition was difficult, since data from literature was limited.

3.2 Particle size distribution

The PSD has been carried out for two different samples: the secondary sludge and the digested sludge. All samples have been collected at the WWTP Delfluent in Harnaschpolder. For the secondary sludge samples two types have been used which differ in solid content. The non-thickened sludge with 6 g/kg (0.6 wt% DM) and thickened sludge, concentrated 10 times, thus 60 g/kg (6 wt% DM). It should be noted that the DM of the secondary sludge samples were not measured at the WWTP. The values of 0.6 wt% DM and 6 wt% DM were the *expected* values given by (Weij, 2017). The exact compositions have been determined in section 4.4. Further in the report the samples will be referred to as non-thickened and thickened (secondary) sludge.

The digested sludge consists of a 50/50 mixture of primary and secondary sludge. At the outlet of the digester the solid content is 30-40 g/kg (3-4 wt% DM). The dewatered digested sludge, also investigated, has solid content of 220-240 g/kg (22-24 wt% DM). Both DM concentrations are monitored within the WWTP. Further in the report the samples will be referred to as digestate and dewatered digestate.

To identify the rheological properties first the PSD is determined. This step helps to select the geometry of the rheometer.

The PSD has been measured using a Microtrac S3500 model blue wave. The technology is based on laser diffraction in which three red laser diodes characterize the particles. For the experiments a range of 0.0107 – 2000 µm has been used. The data is shown in both a chart and a table including the sizes and percentiles, which can be exported to excel. The flow rate of the machine is represented in percentages of which the highest flow rate, 100%, corresponds to approximately 65ml/s (Gaitan, 2017). Based on advice of the LAB technician the flow rate selected within the range of 30-50%. The residence time of each measurement needs to be sufficiently long for all particles to pass the laser at least once. Also, the flow rate should not be too low to prevent sedimentation of the particles. The flow rate should also not be too high since to prevent destruction of particles resulting in smaller particles.

In order for the system to accurately analyse the sludge samples the following settings have been used. The liquid transport medium used was water, since the velocity of light through a medium is material dependent the refractive index is set accordingly. The refractive index of water is 1.333. The system was attached to the tap, thus normal tap-water has been used. The measured particles were defined as sludge with the particle characteristics of absorbing (transparency) and irregular shape. The size range in microns could not be modified. The standard settings are for the upper edge 2000 microns and the lower edge 0.0107 microns.
Each test took three runs of which the average led to the final result.

To transfer the sample into the container of the PSD a spatula has been used instead of a pipet. This was done to prevent that the large particles were blocked at the inlet of the tip. For the rheometer a pipet has been used, but part of the tip was removed to enlarge the opening.

3.3 Rheology

The rheological properties were investigated with the Anton Paar MCR302 modular compact rheometer. This meter has a Peltier-controlled hood for temperature control which allows a range of temperatures between -5 and 200ºC. The accuracy of the machine is controlled by monitoring the torque. For rotational experiments the torque needs to be in the range of 1 nNm – 200 mNm. For oscillating experiments this range varies from 0.5 nNm – 200mNm. All data shown has been carried out within the accepted torque range, unless stated otherwise. An overview of the detection limits for the MCR 302 is shown in Appendix A in Table A.1.

For the rheological properties the most interesting features to be measured are the viscosity and shear stress. Both can be measured under different shear rate conditions and different temperatures. The equipment also allows for the determination of thixotropic behaviour.

In general, three types of geometry are often used: the bob-cup, cone-plate and the plate-plate configuration. The bob-cup configuration, also referred to as concentric cylinder, spindle or couette, is often used for low viscous products whereas viscous products are often tested by the cone-plate or plate-plate geometry.
A schematic overview of the different geometries is given in Figure 3.1.

The experiments were carried out with the B-CC27. This configuration has the bob-cup geometry, Figure 3.1a. The product specifications are represented in Table 3.1. The CC27 is designed for viscosity values in range of 100-1000 mPas (Annaert, 2017). Outside this viscosity range the results are still reliable once the torque remains within the indicated limits.
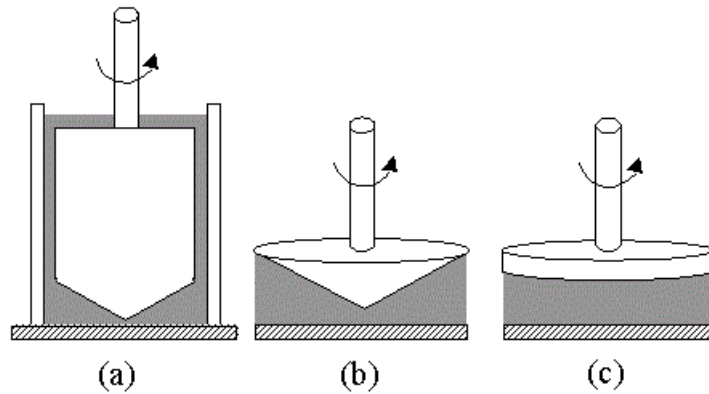
Figure 3.1: Different geometries of the rheometer; bob-cup (a), cone-plate (b) and plate-plate (c) (Hackley and Ferraris, 2001)

Table 3.1 Product specifications of measuring cylinder B-CC27

Type	Diameter [mm]	Cup diameter [mm]
Cylinder (concentric)	26.66	28.92

The B-CC27 is a narrow-gap cylinder and its shear gap dimension is defined according to the ratio δ_{cc} which is specified as the ratio between the bob radius R_i and the cup radius R_e. In order to achieve shear rate values as constant as possible within the entire shear gap, the ISO standard indicates the permissible maximum value of the ratio δ_{cc} which is specified as follows:

$$\delta_{cc} = \frac{R_e}{R_i} = 1.0847; \quad \left(\frac{R_i}{R_e}\right)^2 = 0.85 \tag{3.1}$$

In Table 3.2 it can be observed that the B-CC27 is exactly within the limits of the ISO standard.

Table 3.2: The ratio of the radii of cup and bob, and gap dimension of the B-CC27

R_i [mm]	R_e [mm]	δ_{cc} [-]	Gap ($R_e - R_i$) [mm]
13.33	14.46	1.0847	1.13

The B-CC27 is frequently used for rheology experiments for sludge and clay samples in the Waterlab of Civil Engineering at TU Delft. The sample size of this set-up is approximately 15ml. It should be noted that gap between cylinder and cup is small. In order to have accurate results the distance between wall and cylinder should be at least 10 times larger than the largest particles in the sample. When this requirement is not met, noise in the data could be observed in the form of outliers or unexpected shape of the graph.

3.3.1 Shear viscosity

The first tests which were carried out are indicated as "shear viscosity tests", which is one of the testing options of the rheometer. This test allows for measuring the correlation between shear rate with the viscosity, shear stress and the torque. In addition, the temperature effect has been investigated. The temperature of the sample is controlled inside the rheometer and the samples were tested at different temperatures ranging from 20ºC up to 60ºC as standard. Also, the reversed effect has been studied, going from higher temperatures to lower temperatures. Heating may affect physical properties, since internal structures could change by elevated temperatures.

Initially, the range of the shear rate was set from 1 s^{-1} to 100 s^{-1} and for every measurement a set of 40 data points was collected. The time in between each data point was not taken constant, first it was set to 10 s to be able that the bob was able to rotate fully for a few cycles at low shear rate. Towards the end of the measurement the time in between each data point was set to 1 s. For these steps either a linear scale as logarithmic scale could be used.

To check for hysteresis a simple adjustment of the set-up was made. Instead of going only one way from 1 s^{-1} to 100 s^{-1}, the reverse direction was carried out immediately afterwards and 40 data points were collected in this direction.

Two different shear viscosity tests were set-up, one with pre-mixing and one without pre-mixing inside the cylinder. For the non-thickened sludge sample it was desirable to mix the samples shortly right before the start of the experiment since the solid particles easily sediment. The other sludge and digestate samples were a lot thicker and therefore it was decided not to pre-mix the sample. However, before filling the sample from the container in the cylinder the bottle was well mixed.

During the experiments signs of yield stress appeared. However, determining the yield stress is not an easy task as explained by (Cheng, 1986), who proposed several methods which may lead to different outcomes. In terms of shear viscosity tests two types of yield stress are usually identified: the shear stress value measured at a very low shear rate also named as *static yield stress* and the value obtained by extrapolating the flow curve to intersect with the ordinate indicated as the *dynamic yield stress* (Gurung et al., 2016). The static yield stress has been defined through experiments with an initial shear rate of 0.01 s^{-1} with the duration of the initial data point of 100 s, to make sure that one rotation was performed. It has been decided to start with a shear rate of 0.01 s^{-1}, since experiments at lowers shear rates would take hours.

After some trial experiments it was possible to analyse the static yield stress and hysteresis for different temperatures in one experiment. The followed procedure for the shear viscosity test is shown in Table 3.3. This experiment is carried out at different temperatures.

Table 3.3: Settings rheometer for shear viscosity test

Set-up
1. Set temperature to desired value, for example 20ºC
2. Interval 1 10 data points Duration: initial 100 s, final 1 s, ramp logarithmic scale Shear rates: initial 0.01 s^{-1}, final 1 s^{-1}, ramp logarithmic scale
3. Interval 2 40 data points Duration: initial 10 s, final 1 s, ramp logarithmic scale Shear rates: initial 1 s^{-1}, final 100 s^{-1}, ramp logarithmic scale
4. Interval 3 40 data points Duration: initial 1 s, final 10 s, ramp logarithmic scale Shear rates: initial 100 s^{-1}, final 1 s^{-1}, ramp logarithmic scale

3.3.2   Geometry

For the first set of experiments as mentioned earlier in section 3.3, the measuring cylinder B-CC27 has been used. However, from the PSD results which will be later discussed in section 4.2, it became clear that both sludge and digestate samples do not comply with the standard for distance between wall and cylinder to be 10 times larger as the largest particle size. Therefore, it has been suggested to run experiments using a different geometry. However, the cone-plate has an even smaller gap of 102 µm and the plate-plate is not suitable for sludgy materials. Yet, another not often used geometry was available in the lab named the Building Material Cell (BMC).

The BMC has a cup diameter of 74mm and is specifically designed for rheological measurements on building materials with large particles with sizes up to 5 mm. Building materials show tendencies of wall slippage or separation when sheared with conventional measuring systems. Wall slip relieves part

of the shear stress and a lower viscosity appears. This also shows an increased shear thinning behaviour (Black, 2000). The BMC has been designed to eliminate this phenomenon, since it has a modular inset cage with flow breakers which prevents wall slippage and improves mixing effects (Paar, 2016).

The geometry test consists of a theoretical and experimental part. The theoretical part consists of calculations to estimate the occurrence of turbulent flow behaviour. Turbulent flow may affect the accuracy of the results since it leads to an increased flow resistance. The experimental part consists of shear-viscosity experiments with the thickened secondary sludge in the CC and BMC configuration. The BMC has been tested in combination with the CC45, a cylinder with ribbed surface with a diameter of 45mm. The set-up is shown in Figure 3.2. The gap between cylinder and cup was approximately 14.5 mm.

Figure 3.2: Building Material Cell

3.3.3   Dry matter content and viscosity

For this experiment the effect of the DM concentration on the viscosity has been investigated. First a base concentration has been determined via the TS experiment explained in section 3.4. From this start-concentration a dilution series was made. Dilution of a sample is fast, accurate and easier than to concentrate. The sample was diluted 2 times and 4 times and the experiment could be carried out before the results of the TS were available.

The viscosity was measured with the shear-viscosity test with settings from Table 3.3 for temperatures 20ºC, 30ºC, 40ºC and 50ºC. This experiment has been carried out in the BMC.

3.3.4   Structural changes upon temperature and shear

In this test the effect of high temperature and shear on the particle size has been investigated. The experiment consists of two parts.

The first part consists of a shear viscosity test in rheometer with CC configuration. Here the temperature was first increased from 20ºC to 30ºC to 50ºC and for every interval a shear test has been carried out up to a shear rate of 100 s^{-1}. After reaching the 50ºC the temperature has been lowered again to first 30ºC and finally 20ºC at which the same shear tests have been carried out. The results of this test were analysed to see if temperature has an effect on the corresponding shear stress.

The second experiment covered the effect of temperature and shear on the PSD. First the PSD of the untreated thickened sludge and digestate have been analysed with the Microtrac S3500 as explained in section 3.2. Afterwards, three different conditions have been tested independently: temperature, stirring and a combination of both. The treatment of the samples has been done in the rheometer with the CC configuration. The samples were brought to 60ºC and kept at this temperature for 5 minutes. For the stirring the shear rate has been rapidly increased to 100 s^{-1} and kept at this shear

rate for 2 minutes. For the combination experiment the samples first were brought to 60°C for 5 minutes and the samples were mixed at 100 s^{-1} for 2 minutes also at 60°C. After this pre-treatment the samples have been analysed with the PSD-measuring device and the results were compared with the PSD of the fresh samples.

3.3.5 Long-term stability analysis

Sludge and digestate can be classified as dispersions; the material contains more than one phase where the particles are dispersed in water, the continuous phase. It is interesting to know what the effect of storage will be to predict if phase separation would occur upon storage, making the sample inhomogeneous. Dispersions form a physical network, by performing an oscillation test the structural strength can be analysed.

For dispersions (and gels) the long-term stability of the sample can be easily defined with the frequency sweep, since the frequency is the inverse value of time. Long-term behaviour is simulated by low frequencies. For dispersion stability two pre-conditions need to be met, namely the test is performed in the linear viscoelastic range (LVER) and the sample shows a gel-like behaviour which is expressed as G'>G''. The LVER corresponds to the region where, at constant frequency, the structure of the sample shows no significant change. Above the limiting value of the LVER γ_L, the structure of the sample has been irreversibly changed and cannot be used for the frequency sweep.
To define the stability of the samples the G'-values are determined at an angular frequency, $\omega = 0.01$ rad/s. In case G'≥10 Pa the dispersion is considered stable. For G'≤1 Pa, the sample is considered non-stable. For G'-values in between 1 and 10 Pa, further testing is required (Mezger, 2014).

First an amplitude sweep test is carried out to define the LVER and to see if the sample shows a gel-like behaviour. The information about the amplitude sweep and the frequency sweep is based on the Rheology Handbook written by Thomas G. Mezger. This book clearly describes the practical considerations for oscillatory tests (Mezger, 2014).

Amplitude sweep
The amplitude sweep test is an oscillatory test (at constant temperature) where the frequency is kept at a constant value and the amplitude is varied. For this test a shear strain amplitude sweep, also referred to as strain sweep, was applied. The shear strain is represented in the following formula:

$$\gamma^s(t) = \gamma_A * \sin(\omega t) \tag{3.2}$$

Of each oscillation cycle the time period is kept constant, thus ω is constant. The variable strain amplitude is increased over time: $\gamma_A = \gamma_A(t)$, which means that the maximum value of the bob's deflection angle is continuously increased.

For low amplitudes both G'(γ) and G'' (γ) display constant plateaus, usually at different levels and correspond to the LVER. From the obtained data it can be easily observed as a straight line in the plotted data.

The goal of this experiment is to determine γ_L. To do so a combination between the visual and manual analysis has been used. The obtained data can be observed in a measuring curve with the strain amplitude (γ) on the x-axis versus the G'-curve on the y-axis. Both the G' and G'' curves have been plotted. However, for the analysis it is recommended to analyse the G'-function, since this curve usually shows the first deviation from the plateau curve. To support the visual observation the data table could be analysed. For this analysis a tolerated deviation range needs to be defined first. This deviation is often in the order of 3%-10% (Mezger, 2014).

It should be noted that the γ_L found strongly depends on the applied frequency. Testing at higher

frequencies may result in higher values of G' and G''. This is caused by the fact that at higher frequencies many structures exhibit less flexibility and therefore higher rigidity. The sample might be more inflexible and more brittle which again might lead to a lower corresponding limiting value of the LVER.

The specific test used with the rheology software of Anton Paar is the "Amplitude sweep – Linear viscoelastic range, default". This test is suitable for viscoelastic, paste-like and gel-like materials and defines the LVER, critical strain or stress. For the machine settings a constant angular frequency ω of 10 rad/s has been used. This is a frequency selected by many users who perform amplitude sweep tests (Mezger, 2014). It was advised by (Annaert, 2017) to start with a shear strain of 0.01% and based on the results the shear strain could be increased or decreased.

The result has been used to define the settings for the frequency sweep test which will be explained in detail below.

Frequency sweep
Frequency sweep is an oscillatory test at a variable frequency, where the amplitude is kept at a constant value. This test is used to investigate time-dependent deformation behaviour since the frequency is the inverse value of time. For this reason, the short-term behaviour can be expressed by rapid motion at high frequencies and the long-term behaviour by slow motion at low frequencies.

In this context a controlled shear strain will be applied. As shown in the Amplitude sweeps paragraph the shear strain is described as:

$$\gamma^s(t) = \gamma_A * \sin(\omega t) \tag{3.3}$$

In this case γ_A is kept constant and a variable angular frequency is applied, thus ω = ω(t). In other words, the amplitude is kept constant and only the period of time for each oscillation cycle is either increased or decreased.
Before the start of frequency sweep test first the limiting value of the LVER needs to be determined. For this reason, the amplitude sweep always needs to be carried out first to ensure that the measurement is performed within the LVER.

The specific test used with the rheology software of Anton Paar is the "Frequency sweep – strain rate oscillatory" and is defined as the measurement of viscoelastic properties (relaxation behaviour). For this test 16 data points have been taken at different frequencies. The range of angular frequencies varied between 0.01 rad/s (used to define the long-term stability) and 100 rad/s.

3.4   Total solids and organic matter
In section 3.2 it was mentioned that the TS fraction of the thickened secondary sludge sample was estimated at 6 wt% and the digestate samples between 3-4 wt%. In order to validate these values the TS and determination of OM have been defined according to the standard method (Clesceri et al., 1999). This method has been slightly adjusted. The new protocol for TS in combination with OM can be found in Appendix A.

In total two batches of thickened sludge and digestate were tested in triplicate. The collection time between the batches was a week. It was expected that the digestate would not show much difference since the residence time in the digester involves 20 days. For the secondary sludge it was expected to find a TS fraction of around 6 wt%. Furthermore, it was hypothesized that the OM for secondary sludge was higher than for digestate due to the conversion process upon AD. Finally, it was presumed that the different batches would result in the same OM.

3.5 Modelling of the results

The results of the rheometer experiments can be used to fit in existing transport phenomena models to describe the observed behaviour. There is a wide variability of models available. The first model that has been used is the Ostwald-de Waele model. This model is simple, but can be applied for Newtonian and non-Newtonian fluids. The model is represented by the following formula:

$$\tau = K\,\gamma^n \tag{3.4}$$

With,

τ: the shear stress [Pa]
K: a constant [-]
γ: the shear rate [1/s]
n: a constant [-]

The value of n immediately indicates the behaviour of the fluid, since n<1 for pseudoplastic, n=1 for Newtonian fluid, n>1 for dilatant.

The model has some limitations; at a shear rate of 0 the shear stress is always 0. Fluids exposing a yield stress cannot be captured in this model. Another problem is that for n<1 the viscosity will become 0 for infinitely large shear rates, in practice a real fluid has both a minimum and a maximum effective viscosity.

Another model which does take the presence of yield stress into account is the Herschel-Bulkley model. This model is very similar to the Ostwald-de Waele model with the only difference being the incorporation of τ_0 which represents the yield stress at a shear rate of 0. Thus,

$$\tau = \tau_0 + K\,\gamma^n \tag{3.5}$$

To conclude whether the model is a good representation an error function has been defined which describes the relative error. The error function is expressed as followed:

$$error = \frac{1}{N} * \sum \frac{\left(y_{fit} - y\right)^2}{y^2} \tag{3.6}$$

Here y_{fit} is the model function, y represents the measured values and N is the sample size. This function makes use of the sum of squared errors. In order to calculate the relative error the sum of squared errors is divided by y^2 in this way the effect of the actual quantity of y is cancelled out. Division by y^2 is necessary otherwise the error would be affected by the unit chosen e.g. mPa would then lead to a larger error than Pa. The total sum of squared errors also needs to be divided by the sample size, otherwise the more observations taken the larger the error. This way experiments with different amounts of data points can be compared.

4   Results and discussion

In this chapter, the results of the experiments and the literature study are described.

4.1   Determine feedstock composition

In Table 4.1 the composition of the chemical composition of different samples is represented. Not all characteristics were found in the same paper. Some feedstocks have blanks in the table and/or are listed double when values are found from different sources.

The chemical composition is defined according to the following parameters:
TS: also indicated as dry matter, the value is expressed in weight percentage of the total mass.
OM: the fraction of the DM which contains organic material.
COD: chemical oxygen demand expressed in grams oxygen per litre.
Nkj: Kjeldahl-nitrogen is the concentration organically bound nitrogen and the ammonium nitrogen expressed in grams per litre.
pH: the acidity gradient.

Table 4.1: Chemical composition of different feedstocks

	TS % (m/m)	OM (% of DM)	COD (g/L)	Nkj (g/L)	pH
Untreated wastewater[1]	0.04-0.12		0.25-0.8	0.02-0.07	
Primary sludge[2]	6.1	68.4	61.2		6.3
Secondary sludge[2]	5.9	71.1	62.1		6.9
Digested sludge Harnaschpolder[3]	3-4	~68			
Biowaste digestate pressed water[4]	25.3	37.5	149.2	5.72	7.2
Biowaste digestate centrate water[4]	12.2	66.2		6.67	7.8
Biowaste digestate centrate water[5]	15	64			
Cattle Manure[6]	8.78		111.0	3.90	
Swine Manure[7]	11.1		159.3	7.26	6.5

Sources: [1] (Temmink and Zeeman, 2015); [2] (Wypkema et al.); [3] (Weij, 2017); [4] (Froeling, 2012a); [5] (Froeling, 2012b); [6] (El-Mashad et al., 2005); [7] (Massé et al., 2000)

From the observed values in can be seen that the values for untreated wastewater are very low. This is caused by the fact that wastewater is a diluted stream, which results in a low DM content. The range of total solid content of wastewater is rather broad. This variation could be caused by weather conditions like rainfall intensity and duration, the wastewater source (industry, households or a combination), the type of sewer system and finally the water consumption of people. Rain fall strongly affects the size and concentration of the influent, therefore at standard conditions a WWTP should not run on full capacity. It can be observed that there is a correlation between TS and the COD of the material, a higher solid content also enables more material to be oxidised. The Nkj values could give an indication of the fraction of proteins present, however it should be noted that ammonium is also part of the measured value.

For the digested sludge in the table it can be observed that the remaining organic matter is around 68% of the DM. This number is retrieved from an analysis of the digested sludge at WWTP Delfluent in Harnaschpolder. Compared to the OM of the primary and secondary sludge measured in 2012 at the WWTP in Bath, this yield seems rather low. However, according to Paul Weij, process engineer at Delfluent, the OM of primary sludge and secondary sludge in Harnaschpolder are more in the order of 75-85% of DM (Weij, 2017).To illustrate the conversion yield of the digester a mass balance has been made, based on the DM and OM of primary, secondary and digested sludge of WWTP Harnaschpolder. The result is shown in Figure 4.1. The quantity of 100kg is only used for the calculation.
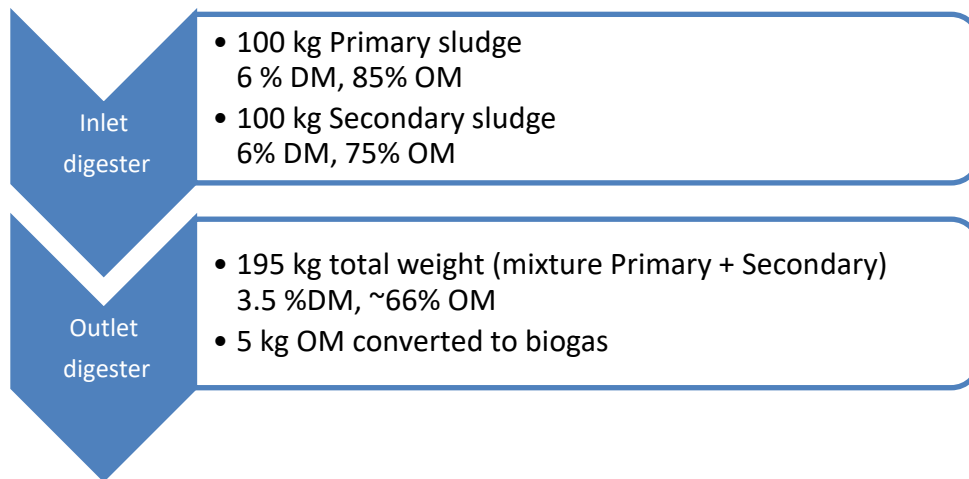
Inlet digester
- 100 kg Primary sludge
  6 % DM, 85% OM
- 100 kg Secondary sludge
  6% DM, 75% OM

Outlet digester
- 195 kg total weight (mixture Primary + Secondary)
  3.5 %DM, ~66% OM
- 5 kg OM converted to biogas

Figure 4.1: Mass balance over a digester used at a WWTP, DM and OM are based on WWTP Harnaschpolder (Weij, 2017)

In subsection 2.4.1 it became clear that primary sludge is easier digested than secondary sludge. In "Handboek Slibgisting" (English: Handbook for sludge digestion) the fermentability of both primary and secondary sludge is defined for a hydraulic retention time of 20-25 days and expressed as a percentage of OM. For primary sludge the fermentability is around 50-60% and for secondary sludge this value is between 25-50% (Nieuwenhuijzen, 2011).The results of Figure 4.1 showed an overall fermentability of 52%. This means that for both primary and secondary sludge the fermentability is close to the upper limits. In section 4.4 the DM and OM of secondary and digested sludge have been determined experimentally.

For the biowaste digestate two different types of products have been defined, the pressed water and the centrate. Explanation of these two streams can be found back in Figure 2.5. The press water stream leaves the press and is sent to the decanter. The centrate is the process stream which leaves the decanter and is recycled back to the digester (not represented) whereas the other outlet flow of the decanter is prepared for composting. The decanter allows the separation of sand, which results in a lower DM overall, but in a higher fraction of OM which is advantageous for both AD as SCWG.

The second analysis of the feedstock involved the biochemical composition. This composition is defined according to the following parameters:

DM: the dry matter content is expressed as weight percentage of total mass. It presents the remaining fraction after evaporation of water (105ºC for 24 hours).
Protein: the protein fraction is expressed as weight percentage of DM.
Lipids: the lipids/fat fraction is expressed as weight percentage of DM.
Carbohydrates: the carbohydrates fraction is expressed as weight percentage of DM and includes cellulose and hemicellulose.
Cel/Hem: cellulose and hemicellulose are often named together since both are fermentable fibres. In some papers the cellulose and hemicellulose were defined individually. In addition, in some papers they were expressed as a percentage of the total carbohydrates. Here cellulose/hemicellulose fraction is expressed as weight percentage of DM.
Lignin: this fibre constituent is classified as the non-fermentable. Lignin is expressed as weight percentage of DM.
pH: the acidity gradient.

Table 4.2: Biochemical composition of different feedstocks

	DM % (m/m)	Protein (%wt DM)	Lipids (%wt DM)	Carbohydrate (%wt DM)	Cel/Hem (%wt DM)	Lignin (%wt DM)	pH
Primary Sludge[1,2]		19-27	14-34	34-39	26-36	2-9	
Primary Sluge[3]		16.8	13.8	28.9			6.19
Secondary Sludge[3]		28.7	12.2	22.2			6.55
Sludge Digestate[3]		11.5	16.8	7			6.83
Dewatered Sludge Digestate[4]	19.4	2.9	8.0	19.6	5.9	6.2	8.03
Sawdust[4]	84.7	3.6	6.2	24.2	8.9	6.0	5.49
Pig Manure[4]	34.3	1.0	4.4	10.5	5.2	3.3	8.37
Dairy Cattle Manure[5]	14.6	18.3	3.2	53.7	38.5	15.2	6.70

Sources: [1] (Nieuwenhuijzen, 2011); [2] (Pinkse et al., 2016); [3] (Bowen and Keinath, 1985); [4] (Li et al., 2001); [5] (Amon et al., 2007)

The biochemical composition shows strong variation between different feedstocks. It should be noted that the collected data of primary sludge, secondary sludge and sludge digestate from the Bowen & Keinath paper is originated from 1985.

There is a difference in composition of the primary sludge of the Bowen & Keinath paper and of the STOWA report. The fraction of proteins, lipids and carbohydrates appears to be higher in the primary sludge of the STOWA report and as a consequence yields in a higher OM, which is desirable for digestion and further processing of the material. The following suggestions may have contributed to this difference:

1. Compared to 1985 more toilet paper ends up in the wastewater, leading to an increase of cellulose concentration, which also increased the total carbohydrate concentration.

2. The sludge collected for the STOWA could have experienced a better separation of the inorganic (non-digestible) fraction, for example sand could have been removed in an early stage.

3. The sludge collected for the Bowen & Keinath paper comes from a WWTP in the USA, the sludge collected for the STOWA report comes from a WWTP in the Netherlands and is collected more recently. Both time and location could have had an influence. Over time technology has evolved and in addition the Netherlands is state-of-the-art when it comes to wastewater treatment technologies.

It is interesting to observe that the biochemical composition of dewatered sludge digestate strongly varies from the sludge digestate. In the paper of the dewatered sludge little information is given on the origin and production process of the feedstock, thus only suggestions could be made for the difference in composition.

First, the sludge digestate from the paper of Li was collected from the Tai PO sewage treatment plant in Hong Kong whereas the samples from the Bowen & Keinath paper were collected from two WWTPs in the USA. Different diets in the countries could influence the composition of the wastewater. Also, the way how wastewater treatment is carried out may strongly vary between (or sometimes even within) countries.

The difference in pH of both samples could also have played a role for the conversion in the digester. However, the pH of 8.03 of the sludge from Hong Kong is measured after dewatering, thus it cannot be stated that the pH inside the digester also had this value.

In the paper of Bowen & Keinath it was specified that municipal wastewater was used. The paper of Li however did not specify if only municipal wastewater was treated or also wastewater from industries (combined sewer).

When looking at the other sources it is understandable that wood is often used for gasification due to its high DM content, but is not interesting for SCWG since the water fraction needs to be at least 40%. Dairy cattle manure appears to be a suitable source for AD due to the high fraction of cellulose/hemicellulose, but it could also be an interesting source for SCWG.

4.2   Particle size distribution

The first step in the PSD analysis was the selection of the correct flow velocity. In section 3.2 it was explained that the flow velocity is not universal for every sample due to precipitation or degradation of the sample. For non-thickened sludge and digestate experiments have been carried out at different flow rates. The results of this experiment can be found in Appendix 0, Figure C.1 and Figure C.2. For velocities in the range of 30-50% the impact on the performance of the PSD is appears negligible for both the sludge and digestate samples. It has been decided to further experiment with a flow rate of 50%. In total four different samples have been analysed: non-thickened secondary sludge, thickened secondary sludge, digestate and dewatered digestate.

The results of the non-thickened and thickened sludge are shown in Appendix 0, Figure C.1 and Figure C.3. It can be observed that the range of the non-thickened sludge varies from 6.54 – 352 um. For thickened sludge the range is slightly broader from 5.5 – 497.8. This could be caused by different reasons. The samples were not collected on the same date, thus the composition of the sludge could therefor differ. Another explanation is thickened sludge particles showed coagulation caused by the thickening process.

The DM content of the investigated digestate was 3-4 wt%. The dewatered digestate is constantly monitored at the WWTP. The dewatered digestate was collected once and had a DM content of 22.75 wt%. The results of the PSD for the digestate and dewatered digestate are found in Appendix 0, Figure C.2 and Figure C.4 respectively. The digestate samples varied from 5.5 – 704 um. This indicates that the largest secondary sludge particles are significantly smaller than the largest digestate particles. This could be explained by the following: the digestate is composed of a combination of primary and secondary sludge. The primary sludge consists of particles which sunk to bottom of the pre-settling tank, which are usually the larger and heavier particles. The secondary sludge consists of biomass which grows on the dissolved nutrients left in the wastewater.

The dewatered digestate was very difficult to handle since the texture was comparable with clay. This can be observed in a picture of the material shown in Figure 4.2.

Figure 4.2: Dewatered digestate (22.75 wt% DM)

For the PSD different samples of the same batch have been analysed. The results, however, were not consistent as could be observed in Appendix C, Figure C.4. The detection limit of the PSD is 2000 µm.

Two of the three samples reached this detection limit and this could mean that even larger particle sizes were present in the sample. An alternative for determining PSD could be via sieve analysis, which is well suitable for large particles. Ultrasound is another method and is used to analyse particle sizes between about 10nm and 1000 μm (McClements, 2006). However, this detection limit is even lower than for laser diffraction.

The dewatered sludge was very sticky, as shown in Figure 4.2. With the use of a spatula the samples have been transferred to the container of the PSD. Due to the coagulation of particles and exceeding the detection limit, it can be concluded that this sample is not suitable for the B-CC27 for further experiments. The largest particles are even bigger than the gap between bob and cylinder of 1.13 mm. In addition, the material is too viscous for this geometry to be able to perform an analysis.

From Appendix 0, Figure C.2 it can be seen that a large fraction of the particle sizes of the digestate are found in the smaller size region. Even though the digestate is a combination of secondary sludge and primary sludge of which the latter is expected to have bigger particles as explained above. The smaller size region suggests that upon digestion the particles will become smaller. This is in line with the description of the degradation pathway of AD. AD consists of four different steps as shown in Figure 4.3. The biomass entering the digester consists in most cases of large organic polymers like proteins, polymeric carbohydrates, or lipids. For the bacteria to fulfil their function, the long chains first must be broken into smaller constituents. This is done through hydrolysis (splitting with water), which is shown as the first step in the figure. The resulting smaller molecules (amino acids, sugar monomers, long-chain fatty acids and glycerol) will dissolve in water (Kleerebezem, 2014) and could be converted to CH_4 and CO_2 via the acidogenesis, acetogenesis and methanogenesis steps.
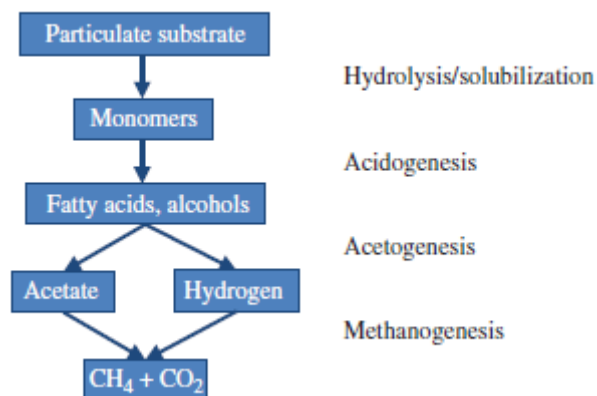

Figure 4.3: Simplified scheme of the sequence of conversion reactions occurring during the anaerobic digestion process (Kleerebezem, 2014)

4.3 Rheology

For the rheometer a series of experiments have been carried out to define the different properties. At first the relationship between shear rate and shear stress has been defined at different temperatures. In this set-up the hysteresis effect has been studied. The effect of geometry on the data has been investigated in order to propose the best experimental set-up Furthermore, the correlation between DM content and viscosity has been identified. These experiments have been followed by testing whether temperature and stirring affect the PSD. Finally, the viscoelastic behaviour of the materials have been studied which also gave information on the long-term stability of the feedstocks.

Four different samples two secondary sludge and two digested sludge samples have been used for the rheology experiment. The results of the PSD from section 3.2 revealed that dewatered digestate with 22.75 wt% was likely to give difficulties in the B-CC27 geometry. As a trial experiment this sample has been diluted with tap-water to 15 wt%. The sample was still relatively solid, a picture of the diluted

sample is shown in

Figure 4.4. This sample has been inserted in the cylinder of the B-CC27. When the bob was lowered into the sample the normal force was 15.08 N as shown in Figure 4.5. This force is considered too high and as a safety procedure the bob did not further penetrate into the sample. Unfortunately the other geometries available, cone-plate, plate-plate and BMC were also not suitable test this material. Therefore, it has been decided to not further experiment with this material.

Figure 4.4: Diluted dewatered digestate (15 wt% DM)

Figure 4.5: Error message rheometer

4.3.1 Shear viscosity

For the shear viscosity tests different results were obtained, the data has been plotted in MATLAB, since this programme has also been used to model the results. The shear viscosity tests have been carried out for three different samples: non-thickened sludge, thickened sludge and digestate.

In Figure 4.6 the relationship between shear rate and shear stress at different temperatures has been investigated for the non-thickened sludge of approximately 0.6 wt% DM. As a reference a tap water at 25ºC has been added.
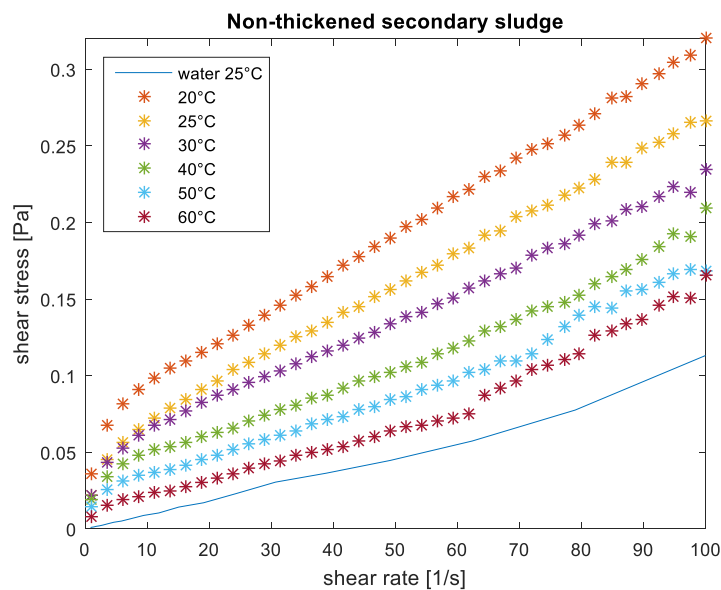
Figure 4.6: Shear rate versus the shear stress for non-thickened secondary sludge sample

Water is a Newtonian fluid and thus obeys Newton's Law:

$$\tau_{xy} = \eta\gamma_{xy} \tag{4.1}$$

Since viscosity remains constant a linear correlation between shear stress and shear rate should be observed. Figure 4.6 shows a linear curve for water. Water at ambient temperature has a viscosity of 1 mPa. According to Newton's law at shear rate 100 s^{-1} shear stress of 0.10 Pa is expected. The shear stress from the figure equals 0.11 Pa, thus close the expected value.
For the non-thickened sludge it can be observed that, although the DM content is still rather low, the impact on the shear stress is significant. The increase of temperature reduces the shear stress. This indicates that operating at higher temperatures could be a useful tool to enhance pumpability.

When comparing the non-thickened sludge data with the different type of fluids shown in Figure 2.6 at first Newtonian behaviour would be considered, since the relationships between shear rate and shear stress seems rather linear. However, another criterion for a Newtonian fluid is that the viscosity is independent of shear. For this reason, the shear rate versus viscosity has been plotted in Figure 4.7. This result shows that viscosity does depend on shear rate and shear thinning/pseudoplastic behaviour is observed. Thus, it can be concluded that the sludge is a non-Newtonian.
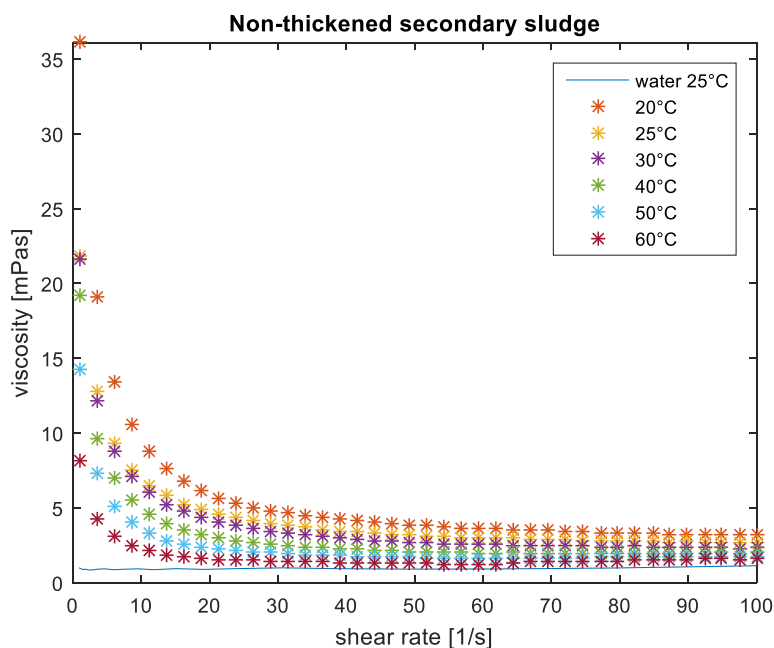
Figure 4.7: Shear rate versus the shear stress for non-thickened secondary sludge sample

It should be noted that samples with DM content below 5% are in general not interesting for the SCWG due to economic feasibility. However, this test reveals that even low DM contents have significant effect on shear stress.

For the next experiment, the digested sludge has been analysed. The result of this test can be observed in Figure 4.8. At first it should be mentioned that the water reference sample has not been plotted in this figure, since its values would not be noticed on a linear scale in Pascal.
Here the correlation between temperature and shear stress is also clearly observed. The graph at 20ºC shows a couple of outliers, this could be caused by the presence of the larger particles. However, since 40 data points have been taken for each temperature the outliers will not dominate the dataset. By analysing the shape of the graphs either *Bingham pseudoplastic* or *pseudoplastic*

behaviour is observed based on the presence or absence of yield stress, which cannot immediately be defined from the plots starting at shear rate 1 s⁻¹. In section 4.5 the model which has been fitted for this dataset will be represented.
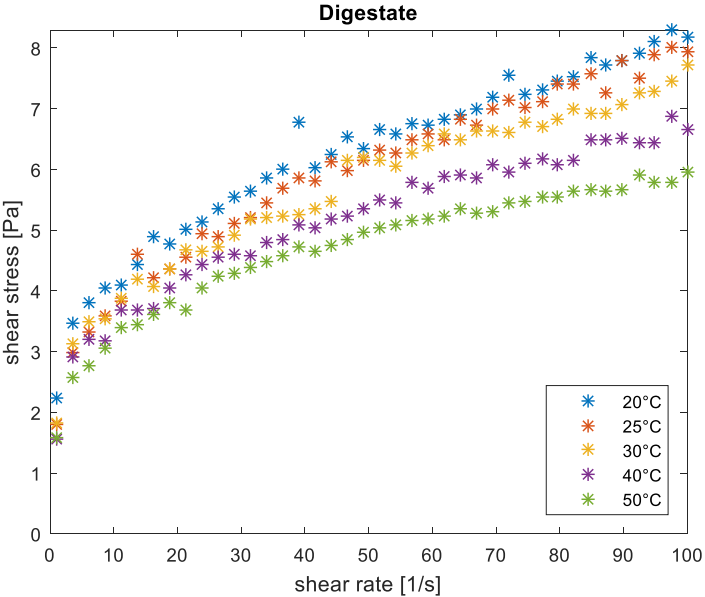

Figure 4.8: Shear rate versus the shear stress for digested sludge sample

For the determination of the static yield stress very low shear rates are applied. First a trial experiment has been carried out with tap water. The results of this experiment are shown in Figure 4.9.
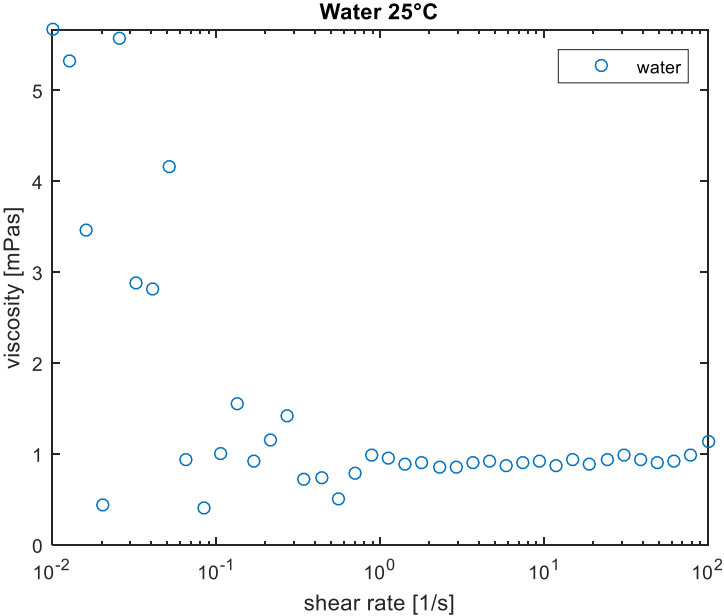
Figure 4.9: Shear rate versus the shear stress for water at 25°C

The shear rate has been plotted on a logarithmic scale in order to show a better visual appearance of data points in the low shear region. The results were actually rather surprising. It was expected that, since water is a Newtonian fluid, the viscosity would remain constant at each shear rate. From the figure it turns out that a broad scatter of values at low shear rates appear. First the corresponding torque values have been analysed. The torque should be within1 nNm – 200 mNm, at the low shear

rates (< 1 s⁻¹) the torque was close to the lower limit and for one data point exceeded this limit. In Figure 4.9 it can be observed that below 1 s⁻¹ the viscosity values indeed start to scatter. The low viscosity of water in combination with low shear rate resulted in critical torque values. Operation outside the recommended torque range appears to be the principal reason of the scattered data. Also, the presence of minor contaminations could have had an impact. In addition, tap water was used instead of demineralised water which may lead to small deviations in the results. To test system calibration the "adjust motor - air check" has been carried out. The output of the calibration test confirmed that the system was well calibrated.

4.3.2 Geometry

This subsection consists of two parts a theoretical and experimental approach.

The theoretical part covers the likelihood of turbulent flow behaviour, leading to an increased flow resistance. This effect can be contributed to the presence of Taylor vortices or exceeding the critical Reynold number. For the CC27 literature was available to calculate their potential. For the BMC it was unclear if the same formulas apply. Therefore, only a suggestion has been made.

Taylor Vortices

For narrow cylinder gap geometries where the bob is rotating and the cup is stationary, there is a critical upper limit between laminar and turbulent flow behaviour at which flow instabilities are occurring, named Taylor vortices. These Taylor vortices result in a secondary flow pattern with large stacked toroidal vortices as can be observed in Figure 4.10.
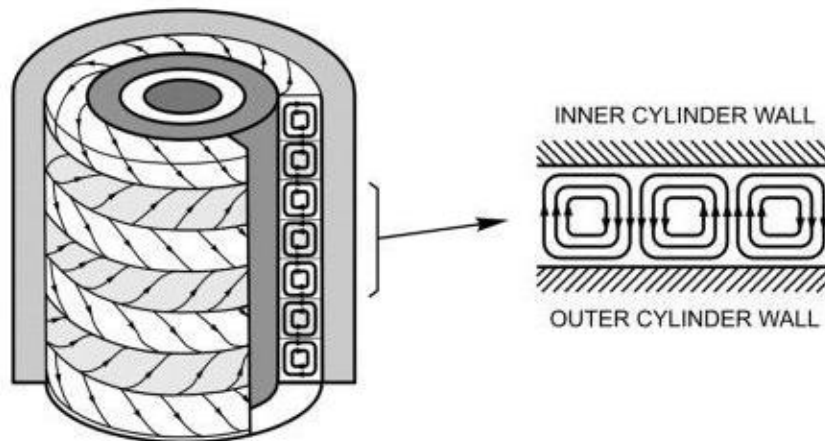

Figure 4.10 Schematic representation of the formation of Taylor vortices between rotating bob and cup (Bizotto and Sabadini, 2008)

For Taylor vortices to occur the critical angular velocity ω_c needs to be exceeded. The critical angular velocity is calculated by the following formula:

$$\omega_c = \frac{41.2 * \eta}{\rho * R_i^2 * (\delta_{cc} - 1)^{\frac{3}{2}}}$$

(4.2)

With ω_c in [rad/s], the viscosity η [Pas], density ρ in [kg/m³], radius of the bob R_i [m] and ratio of the radii δ_{cc}.

In order to calculate the critical shear rate γ_c from the critical angular velocity ω_c in a narrow cylinder gap the constant C_{sr} is introduced. This constant depends only on the ratio of the radii of cup and bob. For the CC27 with δ_{cc} = 1.0847, C_{sr} equals 1.291 (Mezger, 2014).

This results to the following equation:

$$\gamma_c = 1.291 * \frac{\omega_c}{2\pi}$$

(4.3)

The density has not been measured but was based on literature. For secondary sludge with 6% DM the density is 1010 kg/m^3 (Andreoli et al., 2007). The radius of the bob and the ratio of the radii were taken from Table 3.2 and were converted to the correct units.

From the equation, it can be observed that the lower the viscosity the lower the critical shear rate. For the experimental approach, the highest shear rate value corresponds to 100 s^{-1}. Since the sludge shows shear thinning behaviour it is important to find out if the *critical shear rate* is below 100 s^{-1} at the viscosity of the shear rate of 100 s^{-1}. If not, Taylor vortices are not present within the measured shear rate range of 1 to 100 s^{-1}.

The viscosity is based on the sample CC #1 at shear rate 100 s^{-1} of the experimental test, see Figure D.1. The calculated values at different temperatures are represented in Table 4.3.

Table 4.3: Calculation of critical shear rates of the secondary sludge samples in the CC27 at different temperatures

Temperature of sample [°C]	Viscosity at 100 s^{-1} [Pa*s]	Critical angular velocity ω_c [rad/s]	Critical shear rate γ_c [s^{-1}]
20	0.698	6490	1334
30	0.609	5666	1164
40	0.549	5108	1049
50	0.493	4582	941

From Table 4.3 it becomes clear that the critical shear rate will by far not be exceeded and as a result, Taylor vortices are not present in the CC27.

For the BMC it is not clear if the same formula applies, it could be that the formula is different since the surface of wall and cylinder are rough instead of smooth. In case the same formula applies it can be observed that critical angular velocity is lower than for the CC27, since both R_i as δ_{cc} are larger, 0.0225 m and δ_{cc} = 1.56, compared to the values for the CC27. Critical angular velocities will now be in the order of 100 rad/s. Thus, it is likely that the critical shear rate will be exceeded when measurements are carried out in a shear rate range of 1 – 100 s^{-1} and Taylor Vortices could appear.

Reynolds number
Turbulent flow behaviour can also be caused by reaching the critical Reynolds number (Re).
The Reynolds number can be calculated with the following formula:

$$Re = \frac{[\omega * \rho * (R_e^2 - R_i^2)]}{2 * \eta} \tag{4.4}$$

With ω in [rad/s], the viscosity η [Pas], density ρ in [kg/m^3], radius of the bob R_i [m] and the radius of the cylinder R_e [m].

For flow instabilities to occur there two critical Re numbers exist:
1) $Re_{c1} \geq 1$: occurrence of *end effects*, causing flow instabilities around the edges of the upper and lower end of the cylindrical part of the bob.
2) $Re_{c2} \geq 1000$ (to 10,000): occurrence of turbulence in the circular gap itself (Mezger, 2014).

The formula tells that Reynolds number increases for an increase in shear rate and for a decrease of viscosity. For sludge samples the Re number will rapidly increase since higher shear rate and lower viscosity happens simultaneously due to shear thinning behaviour.

In Table 4.4 the Reynolds number is calculated at the shear rates 1 s^{-1} and 100 s^{-1}, the same sample as for the Taylor Vortices has been used for the viscosity. From the table it becomes clear that in no case Re$_{c2}$ is reached. For all temperatures during the shear rate interval Re$_{c1}$ is reached.

Table 4.4: Calculation of Reynolds number for the secondary sludge samples in the CC27 at different temperatures

Temperature of sample [ºC]	Re-number at 1 s^{-1} [-]	Re-number at 100 s^{-1} [-]
20	0.005	11.061
30	0.006	12.670
40	0.007	14.055
50	0.009	15.669

For the BMC the conversion factor for shear rate to angular velocity is not defined, but an estimate calculation has been performed. The Re-number will be higher compared to CC since the gap size of the BMC bigger. For shear rate 1 s^{-1} Re will be around 0.1-0.3, thus below Re$_{c1}$. At 100 s^{-1} the Re-number will be in the order of 200-500, thus above Re$_{c1}$ but below Re$_{c2}$. Thus, the same behaviour could be expected for the BMC as for the CC, although the end effects are likely to appear at lower shear rates for the BMC.

For the experimental part, the results of the CC and BMC have been compared with each other based on the correlation between shear rate and shear stress. In addition, the samples have been tested for the hysteresis effect. In Figure 4.11 the result at 30ºC is shown. Since the same behaviour is observed at all temperatures, the other figures are found in Appendix D. It should be noted that CC #2 has not been tested at 40ºC.
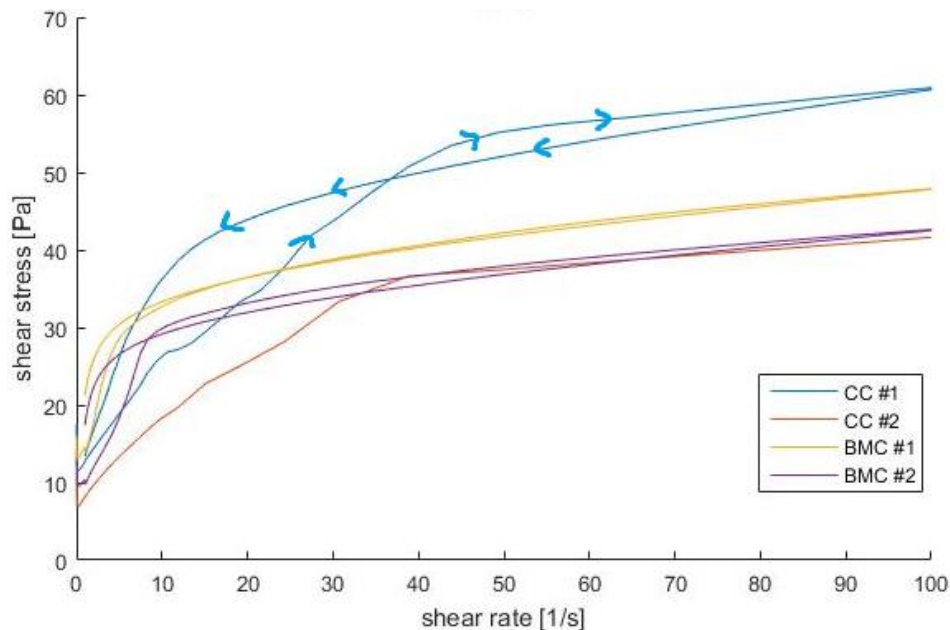

Figure 4.11 Shear rate versus shear stress for thickened secondary sludge at 30ºC, both CC and BMC were tested with two samples, all four samples were collected on different dates, thus may vary in DM content

From the results, the first thing that appears is that shear stress varies for the different samples. This is most likely a result in variation of DM content, since all samples were collected at different times. The shape of the curves of the CC (blue and red) raised some concerns. First of all, both curves are not very smooth, they do not follow the exact shape of one of the curves from Figure 2.6. The CC #1 was tested for hysteresis, indicated with the arrows. The result was unexpected: the reversed flow

shows a higher shear stress. For thixotropic material, material which shows hysteresis, the structure is lost upon shear and it takes time to rebuild its structure (Franck, 2017). As a result, thixotropic material should show a lower shear stress for the reversed flow. The behaviour of the CC #1 would indicate that something went wrong in the measurement. This could be caused by a local concentration difference. For both BMC samples the reversed curve almost overlaps, which shows absence of hysteresis, except for the very lower shear rate region. In which the same problem is observed as for the CC #1 sample, the reversed curve lies on top. This could be caused by wall slip, even though the BMC has been designed to prevent this.

Both geometries do not appear to perform well in the low shear rate regions. At increased shear rate the CC and BMC may experience flow instabilities since the Re_{c1} is exceeded. Overall the BMC resulted in smoother graphs. However, its large gap makes the BMC more sensitive to Taylor Vortices leading to an increased flow resistance.

4.3.3   Dry matter content and viscosity

For this experiment three different DM contents have been tested, 4.72 wt%, 2.36 wt% and 1.18 wt%. The shear rate has been plotted versus the common logarithm (log 10) of the viscosity. All results have been combined in Figure 4.12. The low viscosity for the sample of 1.18 wt% DM at 20ºC directly draws attention. In fact, all results at this concentration are in the opposite direction as expected. Here the viscosity at 50ºC is the highest, whereas this is expected to be the lowest. It could be that the viscosity at 1.18 wt% is on the lower detection limit for the BMC. Nevertheless, the correlation between DM and viscosity has been analysed.

From Figure 4.12 it appears that there is a logarithmic correlation between DM content and viscosity. This has been checked by adding up the values of data points at 4.72 wt% and 1.18 wt% and divide by two. In case the correlation is logarithmic the calculated values will overlap with the values measured at 2.36 wt%. The results of this test are shown in Appendix E, Figure E.1. The model seems to fit with the measured data. Except for the modelled values at 20ºC, which are lower than the actual data. This could be caused by the unexpected low values at the 1.18 wt%.
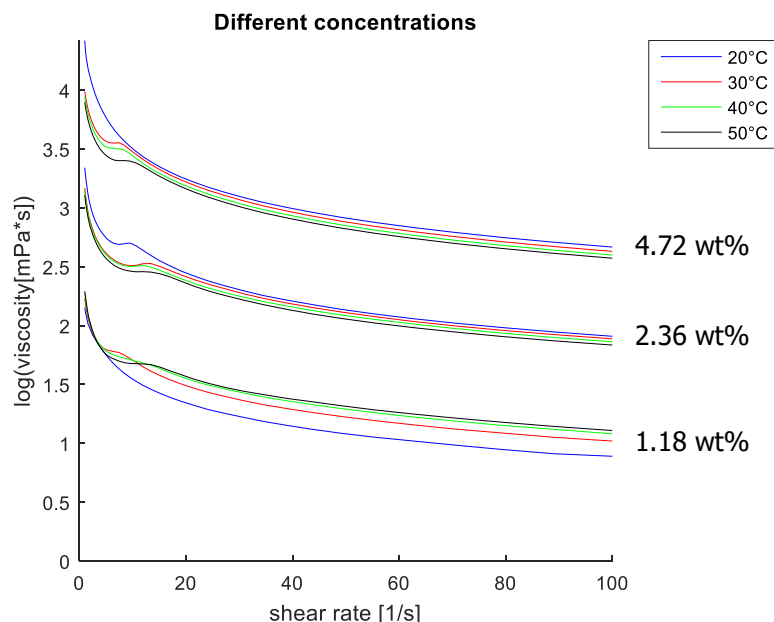

Figure 4.12 Logarithmic viscosity versus shear rate for 4.72 wt%, 2.36 wt% and 1.18 wt% DM at different temperatures

From the results it seems that the viscosity scales logarithmically with the DM content. However, it cannot yet be justified that the same behaviour will appear at higher DM content. Other factors might play a more dominant role at higher DM content like interactions between particles.

4.3.4 Structural changes upon temperature and shear

For the first part of the experiment it has been analysed if the increase in temperature of a sample followed by decrease in temperature affects the corresponding shear stress. Figure 4.13 shows that for both 20ºC as 30ºC there is a clear difference before and after the sample has reached the 50ºC. In the very low shear regions all curves get an unexpected shape. The most likely explanation is the inability of the equipment to perform the test at these low shear rates.
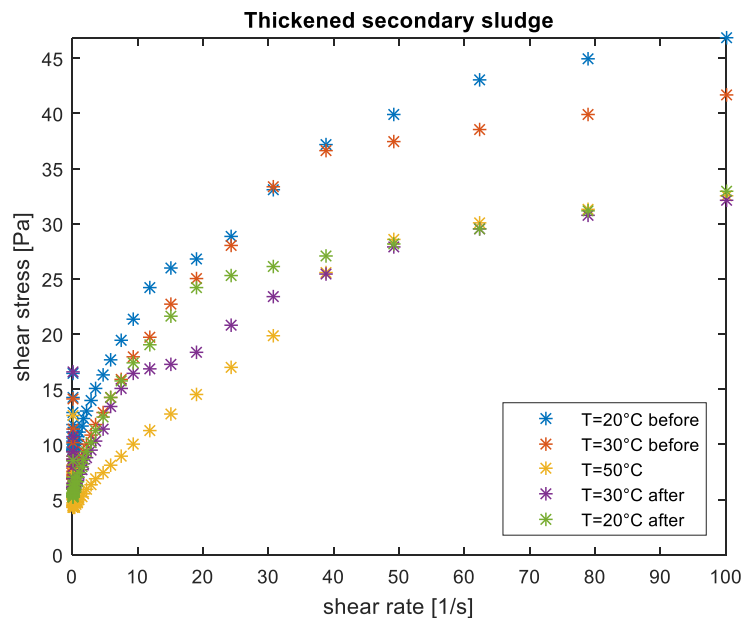
Figure 4.13: Shear rate versus shear stress for thickened secondary sludge for increased and decreased temperatures

Before the cool-down the behaviour of the material is the same as seen before: with increasing temperature, the corresponding shear stress is decreased. However, when cooling down the process turns out not to be completely reversible, since both 20ºC and 30ºC do not overlap with the initial graphs. And this makes it interesting to analyse if temperature and/or shear have an effect on the structure by means of particle size. The different conditions have been tested for both the thickened sludge and the digestate samples. The data is represented in Appendix F. It appears that the PSD does not vary a lot for the different conditions of both the thickened sludge (Figure F.1 and Figure F.2) as the digestate (Figure F.3 and Figure F.4). After a statistical analysis where all conditions are compared with each other it appeared that the error bars are rather small. This indicates that temperature and shear do not significantly affect the PSD. This result was rather surprising, since it was expected that shear would reduce the particle size and that temperature could also lead to degradation of particles. The results of the PSD are only limited to particle size. Effects on morphology have not been investigated, but would be interesting for future research. To analyse the structure and morphology a Scanning Electron Microscope (SEM) could be used (Chang and Morris, 1990). Denaturation of proteins could affect the structure, since it unfolds proteins. The denaturation of proteins usually leads to a reduced water retention also described by the water holding capacity (Van der Sman, 2007). In addition, fibres could have been affected by heating. This could have caused the change in shear stress behaviour.

4.3.5 Long-term stability

The combination of the amplitude sweep and frequency sweep has been used to define the long-term stability of the sample. First, the amplitude sweep has been used to determine the LVER and its limiting value. This value was required for the settings of the frequency sweep test, since this measurement needs to be carried out in the LVER.

Both the long-term stability of thickened secondary sludge and digestate has been analysed. As indicated in subsection 3.3.5 it is recommended to analyse the G'-function. However, the reason that this curve shows the first deviation from the plateau curve does not apply in this situation as can be observed in Appendix G, Figure G.1 and Figure G.2. Both figures show that the G'' values do not reach the plateau. The G' curve was used to define the limiting value of the LVER for the frequency sweep test.

For the thickened sludge sample, Figure G.1, the limiting value of the LVER was defined as a shear strain of 0.243%. Also, it can be observed that G'>G'', which means that the sample behaves as a gel or solid. For the digestate sample, Figure G.1, a shear strain of 0.117% was considered to be the limiting value. For this sample also G'>G'', thus one of pre-conditions for the long-term stability analysis, occurrence of gel-like character, is met for both samples.

The frequency sweep for both samples has been carried out at a shear strain of 0.01%. Thus, a safety factor of at least 10 has been used. The results of the frequency sweep tests can be found in Figure G.3 and Figure G.4. The results of both amplitude sweep and frequency tests were discussed with (Ruijters, 2017). According to Ruijters the chosen shear strain appeared to be correct, the corresponding results were satisfactory and according to him it was not needed to redo the test. Thus this data has been used to analyse the long-term stability.

For stability the value of G' at $\omega = 0.01$ rad/s has been analysed. For the sludge this value equals 138.3 Pa, which means that the dispersion is stable. For the digestate the value equals 22.7 Pa, thus also this sample is considered stable. A possible explanation for the larger G' value of the secondary sludge is the higher DM content. The DM is an indication for the viscosity, a higher viscosity make the sample more stable. To illustrate this, to enhance the stability of a salad dressing, xanthan is added. Xanthan is a stabilizer which increases the viscosity of the dressing. As a result, the dressing remains more homogenous and the particles will not sink to the bottom upon storage.

4.4   Total solids and organic matter

The TS and OM of two different batches of sludge and digestate have been tested. The results were compared with the mass balance from Figure 4.1. In Table 4.5 the results of the measurement are represented. For every sample the average value out of three measurements has been taken.

Table 4.5: TS and OM of different digestate and thickened sludge samples

Sample	TS (%)	OM (%)
Digestate 04-07-2017	3.55	72.9
Digestate 11-07-2017	3.41	73.6
Thickened sludge 04-07-2017	5.39	76.7
Thickened sludge 11-07-2017	4.72	77.0

It can be observed that the TS for digestate of both batches remain between the 3-4%, which is in line with the expectations. For the thickened sludge, however, the values are lower than the expected 6% DM. Also, the variation between the thickened sludge samples is relatively big. This could be explained by weather conditions. Rainfall could have played a role in the concentration of the secondary sludge streams. For digestate composition weather conditions could also play a role, although this effect might be less pronounced since the volume of the digester and the retention time of 20 days make the concentration less sensitive to short-term fluctuations.
In comparison with the mass balance from Figure 4.1 the OM for digestate is lower than the calculated 66%. However, it cannot directly be stated that the conversion yield is lower, since the primary sludge has not been analysed. Overall, it can be concluded that the digestate still has sufficient potential based on OM to function as a feedstock for SCWG.

4.5 Modelling of the results

The model has been based on the digested sludge data, as shown in Figure 4.8. In section 3.5 it was explained that the Ostwald-de Waele model is a useful tool for describing both Newtonian and non-Newtonian behaviour. Therefore, this model has been used to describe the rheological behaviour of the digested sludge.

The digested sludge has been tested at five different temperatures; 20ºC, 25ºC, 30ºC, 40ºC and 50ºC. It is possible to make a fit for every graph individually. However, it would be a lot more interesting if one model could be established describing the behaviour at all five temperatures, in other words to develop a temperature dependent model. Here, the Ostwald-de Waele model is showed again:

$$\tau = K\,\gamma^n \tag{4.5}$$

The parameters K and n are used to describe the shear stress. In order to make the model temperature dependent two options were suggested.
In the first option K is made temperature dependent and in the second option both K and n have been made temperature dependent, resulting in the following two formulas:

$$\tau = \frac{K}{T}\,\gamma^n \quad option\ 1 \tag{4.6}$$

$$\tau = \frac{K}{T}\,\gamma^{\frac{n}{T}} \quad option\ 2 \tag{4.7}$$

It should be noted that the temperature is expressed in Kelvin. In order to test both models, parameter estimation via MATLAB has been carried out including the data of all five temperatures. For the parameter estimation, first an initial guess of K and n has been made via the *polyfit* function. This has been done in order to minimise the number of iterations required for the estimation of K and n. The parameters are estimated with the use of the *lsqcurvefit* function which is used to solve non-linear least squares problems. In Appendix H the MATLAB code for this parameter estimation is represented. The results for option 1 and option 2 are shown in Figure 4.14 and Figure 4.15 respectively.
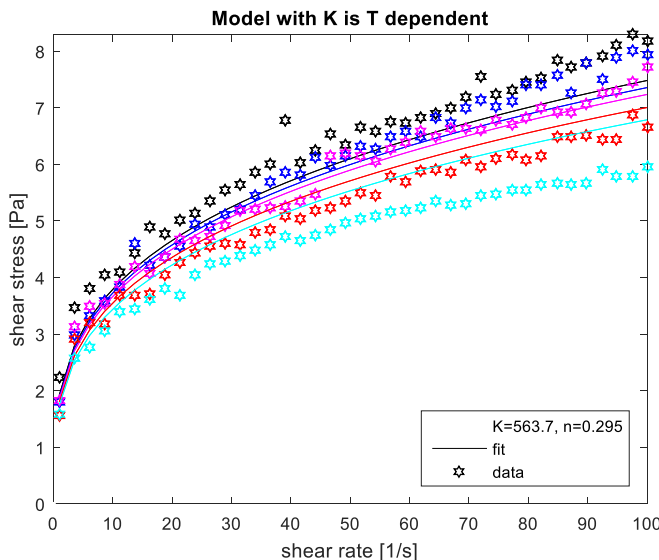

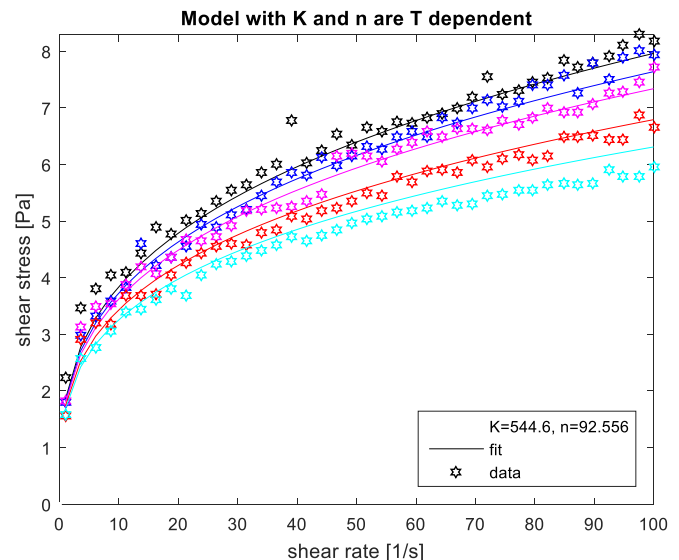**Figure 4.14: Model for 3.4% digestate with K is T dependent**

Figure 4.15: Model for 3.4% digestate with both K and n are T dependent

From the figures it can directly be seen that option 2 gives a better estimation than option 1, which is also expressed via the relative error which is 0.0144 for option 1 and 0.0027 for option 2. Since option 1 does not give a good approximation of the results it has been decided to continue with option 2.

For the estimation in Figure 4.15 the best possible fit for the five different temperatures has been used. However, in order to define whether this model is also suitable to predict the behaviour at other temperatures, again parameter estimation will take place but this time one or more temperatures will be left out of the model fitting. After the new parameters have been estimated the model will be tested at the temperatures which were not used for the parameter estimation. In case the model still matches with the dataset it can be concluded that the model well predicts the shear stress at different temperatures.

To validate the model different set-ups have been used. In the figures the solid lines indicate the temperatures which have been incorporated in the parameter estimation, the dashed lines indicate the test temperatures of the model. For the test conditions the relative error has been defined in order to validate the model. In addition, the values for K and n are compared for the different set-ups.
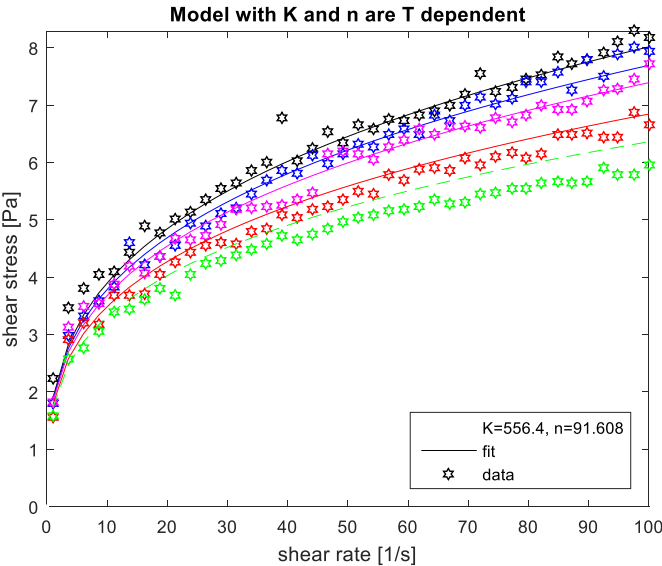
Figure 4.16: Parameter estimation of 3.4% digestate with 20ºC, 25ºC, 30ºC and 40ºC; Test model at 50ºC
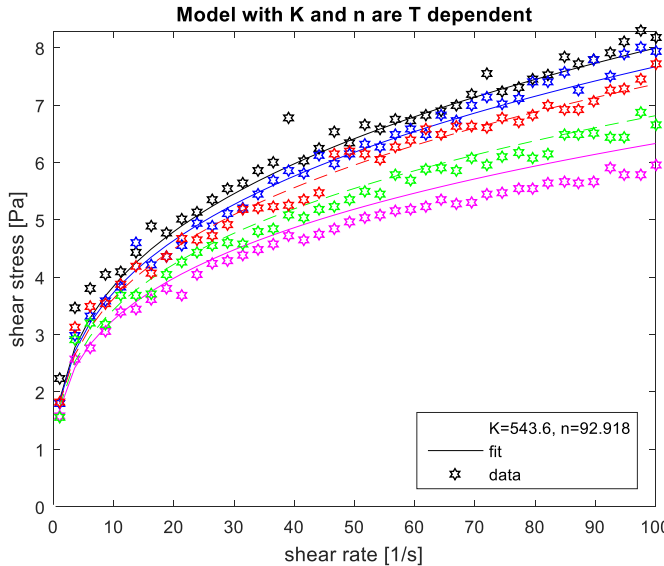
Figure 4.17: Parameter estimation of 3.4% digestate with 20ºC, 25ºC and 50ºC; Test model at 30ºC and 40ºC
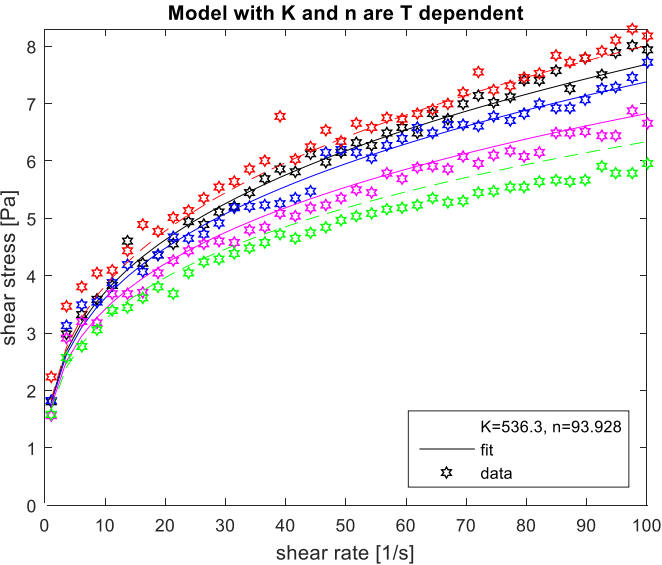
Figure 4.18: Parameter estimation of 3.4% digestate with 25ºC, 30ºC and 40ºC; Test model at 20ºC and 50ºC
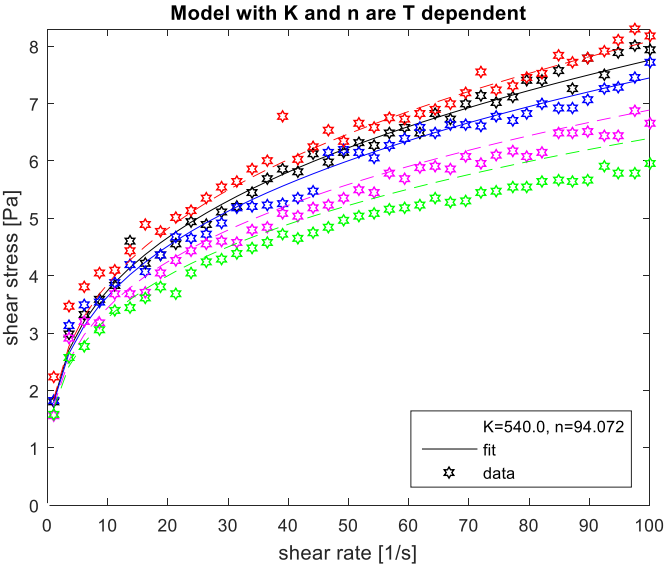
Figure 4.19: Parameter estimation of 3.4% digestate with 25ºC and 30ºC; Test model at 20ºC, 40ºC and 50ºC

In Table 4.6 the different values for K and n and the errors for the different functions haven been represented. Based on the selection of temperatures slight differences in values of K and n are found. Compared to the reference, where all temperatures are used for the parameter estimation, all K-value remains within a range of 2.5% of the reference. The n-values remain within a range of 2% of the reference. The 50ºC appears to be the most difficult temperature to add in this model, since it shows the largest deviation. The relative errors of the validation model remain acceptable, thus it can be concluded that the developed model is a good approximation of the behaviour of the digestate at different temperatures.

The parameter values found for K and n were used to determine the 95% confidence interval. To calculate the confidence interval the following equation has been used:

$$C.I. = \bar{x} \pm Z_{\alpha/2} \frac{\sigma}{\sqrt{N}} \tag{4.8}$$

Here $\bar{x}$ represents the sample mean, $Z_{\alpha/2}$ is the confidence coefficient for the desired confidence level α, σ is the standard deviation and N is the sample size. For the 95% confidence interval $Z_{\alpha/2}$ = 1.96.

For K the 95% confidence interval is 544.2 ± 6.6.
For n the 95% confidence interval is 93.0 ± 0.9.

It should be noted that this confidence interval only applies for the 3.4 wt% digestate, at different DM contents this interval will not apply since K and n will be different. Furthermore, the sample size included only 5 observations. The interval width could be reduced by an increase in sample size.

Table 4.6: Results of validation test of the model of 3.4% digestate

Test	Temperatures for parameter estimation	K	n	Relative error parameter estimation	Relative error validation model
Ref	All temperatures	544.6	92.556	0.0027	
1	20ºC; 25ºC; 30ºC; 40ºC	556.4	91.608	0.0022	50ºC: err = 0.0039
2	20ºC; 25ºC; 50ºC	543.6	92.918	0.0030	30ºC: err = 0.0018 40ºC: err = 0.0016
3	25ºC; 30ºC; 40ºC	536.3	93.928	0.0017	20ºC: err = 0.0037 50ºC: err = 0.0029
4	25ºC; 30ºC	540.0	94.072	0.0016	20ºC: err = 0.0032 40ºC: err = 0.0021 50ºC: err = 0.0038

For modelling of the results it has been decided to use the Ostwald-de Waele model only. In the section 3.5 also the Herschel-Bulkley has been mentioned:

$$\tau = \tau_0 + K \gamma^n \tag{4.9}$$

However, the yield stress is rather difficult to define. Even the method used to determine the yield stress (static and dynamic) could already lead to different results as explained by (Gurung et al., 2016). In addition, the yield stress is a temperature dependent variable. As a result, three parameters of the model would then become temperature dependent. This would make the model unnecessary complex. For this reason, it has been decided to select the Ostwald-de Waele model.

5   Conclusion

The physical properties of secondary sludge and digestate have been characterised in order to improve system performance of the SCWG process, in particular the upstream pumpability of the feedstock. To enhance pumpability the parameters particle size, homogeneity, DM content and viscosity have been investigated.

First different feedstocks have been analysed based on their chemical and biochemical composition. The thickened secondary sludge and digested sludge, both WWTP products, have been used for the experiments based on their centralized and broad availability and the high organic matter fraction, which makes them an interesting feedstock for SCWG.
However, the DM content of both samples is very low: between 4-6 wt% for secondary sludge and 3-4 wt% for digested sludge. On the WWTP the digested sludge is dewatered via centrifugation and polymers are added to achieve a DM content of 22-24 wt%. The polymers make the material clay-like and it was impossible to analyse the sample with the rheometer, which also indicates that it cannot easily be pumped. Therefore, to concentrate the secondary sludge and digestate the addition of polymers should be omitted.

There is no standardized protocol which explains the pumpability limits available, since the interaction between physical properties is material dependent. For particle size, however, the normally tolerated size is 1 mm (LEWA, 2016). The PSD results of thickened sludge and digestate revealed that the largest particles found were 0.5mm and 0.7mm respectively.

For rheology measurements involving large particles, as sludge and digestate, it was found that the building material cell leads to more accurate results compared to the CC27. Although the CC27 is often used, its narrow gap of 1.13 mm interferes with large particles. Data of CC27 and BMC showed that the BMC resulted in smoother graphs with little outliers. Except in the low shear range (< 1 s^{-1}) here, as for the CC27, performance was very poor.

Rheological properties as shear stress and viscosity were affected by temperature and shear conditions. Sludge and digestate showed shear thinning behaviour. In combination with higher temperatures the viscosity and shear stress were further decreased. The PSD was not influenced by increased temperature (60ºC) and stirring at 100 s^{-1}.

A model has been developed to describe the stress as a function of temperature and is based on the rheology data of the digested sludge. The model functions as a convenient tool to predict the temperature influence. The equation originates from the Ostwald-de Waele model and is expressed by the following formula:

$$\tau = \frac{K}{T}\,\gamma^{\frac{n}{T}} \qquad\qquad (5.1)$$

For secondary sludge with low DM content (< 5 wt% DM) a logarithmic correlation between DM and viscosity has been demonstrated. This suggests that viscosity will be the limiting factor for pumpability when the DM content is further increased.

For upstream transportability in the supercritical water gasification process it is desired to decrease the viscosity of the feedstock when possible. It is recommended to store the feedstock in a stirred tank. Aside from effectively decreasing viscosity, stirring also enhances mixing. The feedstock in the tank could be heated, although the effect on viscosity is less pronounced compared to stirring. To avoid evaporation the elevated temperatures need to be kept well below 100ºC.

6 Recommendations

In the following section a collection of recommendations derived from the thesis results are suggested and may stimulate further investigations in this field.

- The rheological experiments have been carried out with the Anton Paar MCR302 rheometer with two different geometries. For both set-ups the performance in the low shear rate zone was very poor. A set-up which accurately measures the shear stress and viscosity at low shear rates of 0.01 s^{-1} or even lower allows the determination of the static yields stress since it simulates the standstill flow. Due to shear thinning behaviour of the sludge and digestate the viscosity of the non-moving mixture is the highest. The maximum allowable viscosity for the stirrer should therefore be based on this value.

- To define the correlation between DM content and viscosity, measurements have been carried out for different concentrations below 5 wt% DM. In order for the SCWG process to be economically feasible the DM content need to be at least 5% (Harinck and Smit, 2014). Therefore, it is imperative to experiment with more concentrated samples. To reduce the water content, a method for water removal needs to be selected. This method should be accurate, preferably not energy intensive and should not alter the product properties. Evaporation therefore would not be suitable, but centrifugation or membrane technology could be. Not only on lab scale but for commercial application a large-scale production of sewage sludge and digestate with increased DM content is desired. It has been found that the addition of polymers at the WWTP alter the physical properties in a way that pumpability becomes impossible. Instead it could be investigated to separate the polymers from the digestate after dewatering or carry out the centrifugation without the addition of polymers.

- In this thesis the rheology experiments have only been tested for short-term temperature effects. In other words, the sample were brought to a specific temperature and measured at that condition. For future research it could be investigated if there is an effect on the rheological properties when the sample is pre-heated, cooled and measured at ambient conditions. In case the pre-heating turns out to be effective it could be beneficial to implement a heating step before the feedstock is pumped to the SCWG system.

- The focus of this project has been on upstream pumpability of the feedstock at atmospheric pressure and mild temperature conditions. The effect of pressure and high temperature on the rheological properties has not been investigated, since the equipment did not allow these conditions. In order to predict flow properties throughout the complete SCWG process experiments need to be carried out with specialised equipment. This equipment can make sub- or supercritical test conditions feasible.

- The biochemical composition of different feedstocks has been analysed via a literature study, but has not been further investigated through experiments. For further research it would be stimulated to investigate the role of proteins, carbohydrates and fats in the physical properties. The biochemical composition could be determined with chemical analyses and the structure and morphology could be investigated with the use of a SEM. The role of these components could help to explain certain phenomena observed, consider denaturation of proteins by heating for example.

References

Acelas, N. Y., López, D. P., Brilman, D. W., Kersten, S. R., & Kootstra, A. M. J. (2014). Supercritical water gasification of sewage sludge: gas production and phosphorus recovery. *Bioresource technology, 174*, 167-175.

Akker, v. d. H. M., R.F. (2014). Stromingsleer *Fysische Transportverschijnselen* (pp. 211-259). Delft: Delft Academic Press /VSSD.

Amon, T., Amon, B., Kryvoruchko, V., Zollitsch, W., Mayer, K., & Gruber, L. (2007). Biogas production from maize and dairy cattle manure—Influence of biomass composition on the methane yield. *Agriculture, Ecosystems & Environment, 118*(1), 173-182. doi:http://dx.doi.org/10.1016/j.agee.2006.05.007

Andreoli, C. V., Von Sperling, M., Fernandes, F., & Ronteltap, M. (2007). *Sludge treatment and disposal* (Vol. 6). London: IWA Publishing.

Annaert, C. (2017, 3-8-2017). [Information about Anton Paar tests and equipment].

Bizotto, V. C., & Sabadini, E. (2008). Poly (ethylene oxide)× polyacrylamide. Which one is more efficient to promote drag reduction in aqueous solution and less degradable? *Journal of applied polymer science, 110*(3), 1844-1850.

Black, W. B. (2000). *Wall slip and boundary effects in polymer shear flows.* University of Wisconsin--Madison.

Boom, R. M. (2015). *Sustainable Food and Bioprocessing* Wageningen: Agrotechnology and Food Sciences Group - Food Process Engineering.

Bowen, P. T., & Keinath, T. M. (1985). Sludge Conditioning: Effects of Sludge Biochemical Composition. *Water Science and Technology, 17*(4-5), 505-515.

Brunner, G. (2009). Near critical and supercritical water. Part I. Hydrolytic and hydrothermal processes. *The Journal of Supercritical Fluids, 47*(3), 373-381. doi:http://dx.doi.org/10.1016/j.supflu.2008.09.002

Chang, M. C., & Morris, W. (1990). The effect of heat treatments on dietary fiber as assessed by scanning electron microscopy. *Journal of Food Processing and Preservation, 14*(5), 335-343.

Cheng, D. C.-H. (1986). Yield stress: A time-dependent property and how to measure it. *Rheologica Acta, 25*(5), 542-554. doi:10.1007/bf01774406

Clesceri, L. S., Greenberg, A. E., & Eaton, A. D. (1999). *Standard Methods for Examination of Water and Wastewater* (20th ed.): American Public Health Association, American Water Works Association, Water Environment Federation.

El-Mashad, H. M., van Loon, W. K. P., Zeeman, G., & Bot, G. P. A. (2005). Rheological properties of dairy cattle manure. *Bioresource technology, 96*(5), 531-535. doi:http://dx.doi.org/10.1016/j.biortech.2004.06.020

Franck, A. (2017). Understanding Rheology of Structured Fluids. *TA Instruments*.

Froeling, D. (2012a). *Analyseresultaten vergisterstromen Zwolle en Middenmeer*. Retrieved from Alkmaar:

Froeling, D. (2012b). Fugaat DS% en OS% *Excel*. Alkmaar: HVC.

Froeling, D. (2012c). *Massabalans Vergister Middenmeer As-built 120301*. Retrieved from Alkmaar:

Gaitan, C. (2017). [Flow velocity of the Microtrac Bluewave].

Gary, D., Morton, R., Tang, C.-C., & Horvath, R. (2007). The Effect of the Microsludge™ Treatment Process on Anaerobic Digestion Performance. *Proceedings of the Water Environment Federation, 2007*(17), 1724-1738. doi:10.2175/193864707788116455

Gensos. (2015). Supercritical Gasification.

Gensos, B. V. (2017). Simplified process flow diagram.

Gurung, A., Haverkort, J., Drost, S., Norder, B., Westerweel, J., & Poelma, C. (2016). Ultrasound image velocimetry for rheological measurements. *Measurement Science and Technology, 27*(9), 094008.

Hackley, V. A., & Ferraris, C. F. (2001). Guide to Rheological Nomenclature: Measurements in Ceramic Particulate Systems. *Special Publication 946*.

Harinck, J., & Smit, K. G. (2014). Process for the gasification of wet biomass: Google Patents.

Heinberg, R., & Mander, J. (2009). *Searching for a Miracle: 'net Energy' Limits & the Fate of Industrial Society*: Post Carbon Press.

Hicks, C. T. (1988). Diaphragm pump: Google Patents.

IAPWS. (2007). *Revised Release on the IAPWS Industrial Formulation 1997 for the Thermodynamic Properties of Water and Steam*. Retrieved from Lucerne: http://www.iapws.org/relguide/IF97-Rev.pdf

IEA. (2014). *World: Balances for 2014*. Retrieved from
https://www.iea.org/statistics/statisticssearch/report/?country=WORLD&product=balances&year=2014

Kersten, S. R. A., & de Jong, W. (2014). Thermochemical Conversion *Biomass as a Sustainable Energy Source for the Future* (pp. 298-358): John Wiley & Sons, Inc.

Kleerebezem, R. (2014). Biochemical Conversion *Biomass as a Sustainable Energy Source for the Future* (pp. 441-468): John Wiley & Sons, Inc.

Korving, L. (2016). *Experimenteel onderzoek superkritisch vergassen van zuiveringsslib*. Retrieved from Amersfoort:

Kosseva, M. R. (2013). *Food Industry Wastes: Chapter 3. Sources, Characterization, and Composition of Food Industry Wastes*: Elsevier Science.

Lee, R. A., & Lavoie, J.-M. (2013). From first- to third-generation biofuels: Challenges of producing a commodity from a biomass of increasing complexity. *Animal Frontiers, 3*(2), 6-11. doi:10.2527/af.2013-0010

LEWA (2016). [Pump requirements for supercritical water gasification].

Li, G., Zhang, F., Sun, Y., Wong, J. W. C., & Fang, M. (2001). Chemical Evaluation of Sewage Sludge Composting as a Mature Indicator for Composting Process. *Water, Air, and Soil Pollution, 132*(3), 333-345. doi:10.1023/a:1013254815976

Massé, D. I., Lu, D., Masse, L., & Droste, R. L. (2000). Effect of antibiotics on psychrophilic anaerobic digestion of swine manure slurry in sequencing batch reactors. *Bioresource technology, 75*(3), 205-211. doi:http://dx.doi.org/10.1016/S0960-8524(00)00046-8

McClements, D. J. (2006). Ultrasonic measurements in particle size analysis. *Encyclopedia of analytical chemistry*.

McKendry, P. (2002). Energy production from biomass (part 3): gasification technologies. *Bioresource technology, 83*(1), 55-63. doi:http://dx.doi.org/10.1016/S0960-8524(01)00120-1

Mezger, T. G. (2014). *The Rheology Handbook* (4 ed.). Hanover: Vincentz Network.

Möller, K., & Müller, T. (2012). Effects of anaerobic digestion on digestate nutrient availability and crop growth: A review. *Engineering in Life Sciences, 12*(3), 242-257. doi:10.1002/elsc.201100085

Möller , M., Nilges , P., Harnisch, F., & Schröder, U. (2011). Subcritical Water as Reaction Environment: Fundamentals of Hydrothermal Biomass Transformation. *ChemSusChem, 4*(5), 566-579. doi:10.1002/cssc.201000341

Moran, M. J., & Shapiro, H. N. (2006). *Fundamentals of engineering thermodynamics* (5th ed.): John Wiley & Sons.

Nieuwenhuijzen, A. v. (2011). *Handboek slibgisting* (9057735229). Retrieved from Amersfoort:

Paar, A. Specifications MCR xx2.

Paar, A. (2016). Extended Material Characterization *www.anton-paar.com* (pp. 12): Anton Paar.

Pinkse, H., Reijken, C., Kras, R., Koot, D., Adriaanse, M., Bult, B., & Uijterlinde, C. (2016). *Verkenning haalbaarheid terugwinning cellulose uit primair sib*. Retrieved from Amersfoort:

RheoSense (Writer). (2015). Viscosity Fundamentals Webinar: Newtonian & non-Newtonian [Youtube]. In RheoSense (Producer), *Viscosity Fundamentals*.

Ringoot, D., & Reitsma, B. N., Remmie. (2014). Thermische hydrolyse als de motor voor centrale slibverwerking. *H2O*.

Ruijters, H. (2017, 31-07-2017). [Information on results and settings of Anton Paar rheometer].

Rulkens, W., & Wentink, J. (2013). *Kan superkritische oxidatie van zuiveringsslib een alternatief zijn voor superkritische vergassing?* Retrieved from Amersfoort:

Sanitary-Engineering, S. (2016). *Wastewater Treatment*. Delft: TU Delft.

Temmink, H., & Zeeman, G. (2015). Water Treatment. *ETE-21306*. Wageningen: Wageningen University.

Van der Sman, R. (2007). Moisture transport during cooking of meat: An analysis based on Flory–Rehner theory. *Meat science, 76*(4), 730-738.

van Lier, J., & de Kreuk, M. (2016-2017). CTB3365STx Treatment of Urban Sewage [MOOC]. Delft: DelftX.

Venema, P., & Sagis, L. M. C. (2012). *Food Physics*. Wageningen: Laboratory of Physics and Physical Chemistry of Foods.

Weij, P. (2017). [Sludge compostion data].

Wypkema, E., Vingerhoeds, R., Colsen, J., & Smet, D. Pilotonderzoek thermofiele slibgisting op rwzi Bath: veelbelovende resultaten.

Yakaboylu, O., Harinck, J., Smit, K., & de Jong, W. (2015). Supercritical water gasification of biomass: A literature and technology overview. *Energies, 8*(2), 859-894.

Zhai, Y., Wang, C., Chen, H., Li, C., Zeng, G., Pang, D., & Lu, P. (2013). Digested sewage sludge gasification in supercritical water. *Waste Management & Research, 31*(4), 393-400. doi:doi:10.1177/0734242X12471097

A Detection limits MCR 302

Table A.1 Specifications of MCR xx2 series (Paar)

	Units	MCR 52	MCR 102	MCR 302	EC-Twist 502	MCR 502 TDR
Bearing		mechanical	air	air	air	air
Min. torque rot.	nNm	200 µNm	5	1	100	1
Min. torque osc.	nNm	200 µNm	7.5	0.5	50	0.5
Max. torque rot./osc.	mNm	200	200	200	300	230
Torque resolution	nNm	100	0.5	0.05	0.2	0.05
Deflection angle (preset)	µrad	1 to ∞	1 to ∞	0.05 to ∞	0.05 to ∞	0.05 to ∞
Internal angular resolution	nrad	10	10	<10	<10	<10
Min. angular velocity	rad/s	10^{-4}	10^{-8}	10^{-9}	10^{-9}	10^{-9}
Max. angular velocity	rad/s	314	314	314	314	314
Step rate, time constant	ms	10	5	5	5	5
Step strain, time constant	ms	10	10	10	10	10
Step time speed (99 %)	ms	30	30	30	30	30
Step time angle (99 %)	ms	30	30	30	30	30
Min. angular frequency	rad/s	10^{-3}	10^{-7}	10^{-7}	10^{-7}	10^{-7}
Max. angular frequency	rad/s	628	628	628	628	628
Normal force range	N	-	0.01 - 50	0.005 - 50	0.01 - 70	0.005 - 50
Normal force resolution	mN		1	0.5	1	0.5

B Total solids and organic matter protocol

Protocol made by Joanne Siccama

Step 1
Collect the number of aluminium cups to perform the test in triplicate. Mark all the cups by scratching in them and measure their empty weight based on four digits behind the comma (Weight 1).

Step 2
Add 10 mL of sample with a 10 mL pipet in each aluminium cup. If necessary, cut off a small part of the tip to prevent blockage caused by large particles. Measure the weight of aluminium cup with sample (Weight 2).
Note: Due to the thickness and large particles in the material it could be possible that not exactly 10 mL of sample will reach the aluminium cup. This causes the TS and OM to only be accurately expressed as weight percentage instead of per volume.

Step 3
Place samples in stove at 105°C for 12 hours.
Note: 24 hours is often recommended. However, for a sample of 10 mL with a large surface area, 12 hours are sufficient to define the TS.

Step 4
After at least 12 hours put samples in desiccator for 10-15 minutes. Afterwards measure the weight of aluminium cup with sample (Weight 3).

Step 5
Place samples in stove at 550°C for 2 hours.

Step 6
After 2 hours put samples first in stove of 105°C for 5 minutes. Careful samples are very hot!
Next transfer the samples to the desiccator for 10-15 minutes. Afterwards measure the weight of aluminium cup with sample (Weight 4).

Step 7
From the measured weights the TS and OM expressed as weight percentage can be defined with the following formulas:

$$TS\ (wt\%) = \frac{Weight\ 3 - Weight\ 1}{Weight\ 2 - Weight\ 1} * 100$$

$$OM\ (wt\%) = \frac{Weight\ 3 - Weight\ 4}{Weight\ 3 - Weight\ 1} * 100$$

C   Results particle size distribution
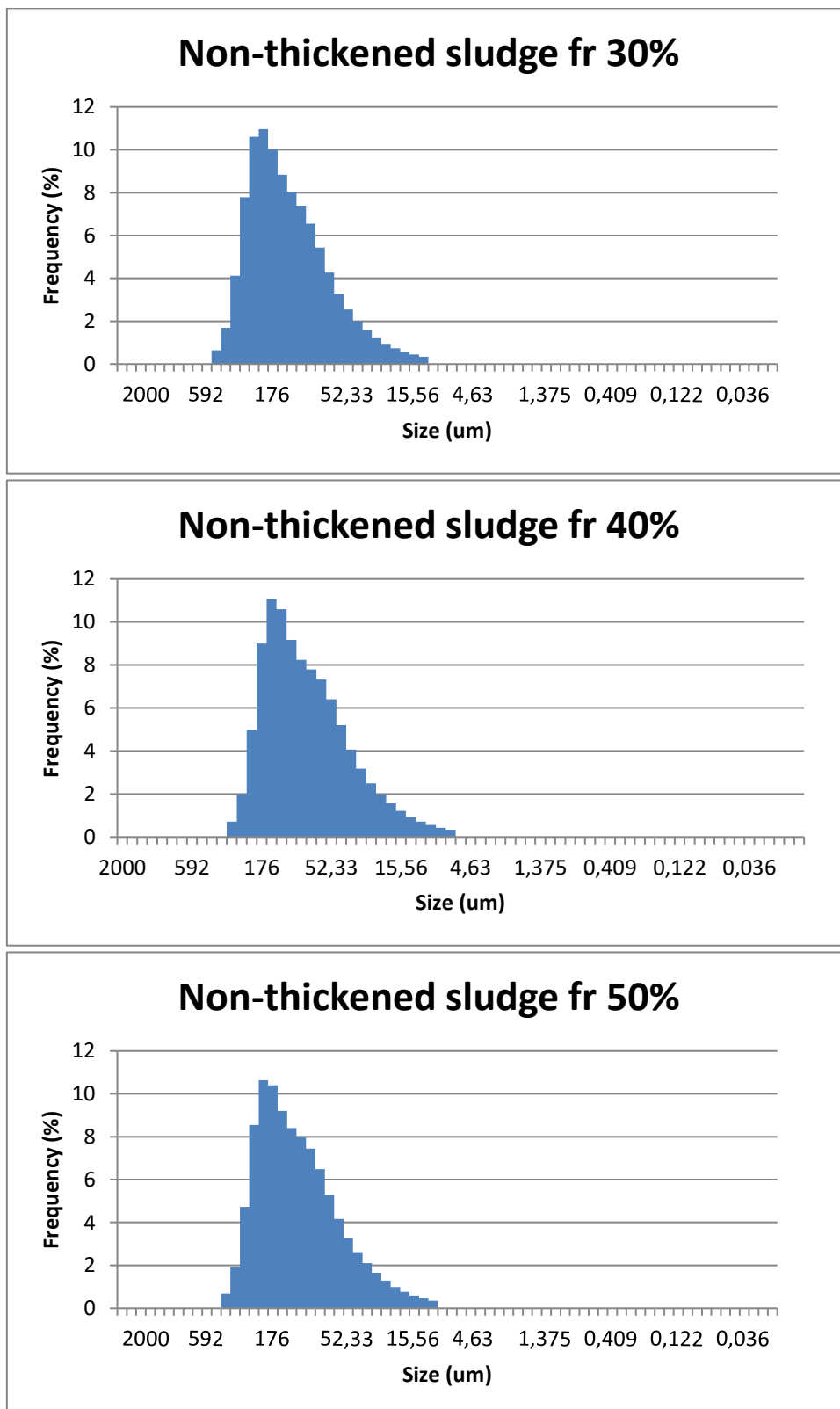
Figure C.1: PSD of non-thickened secondary sludge at 3 different flow rates (fr)
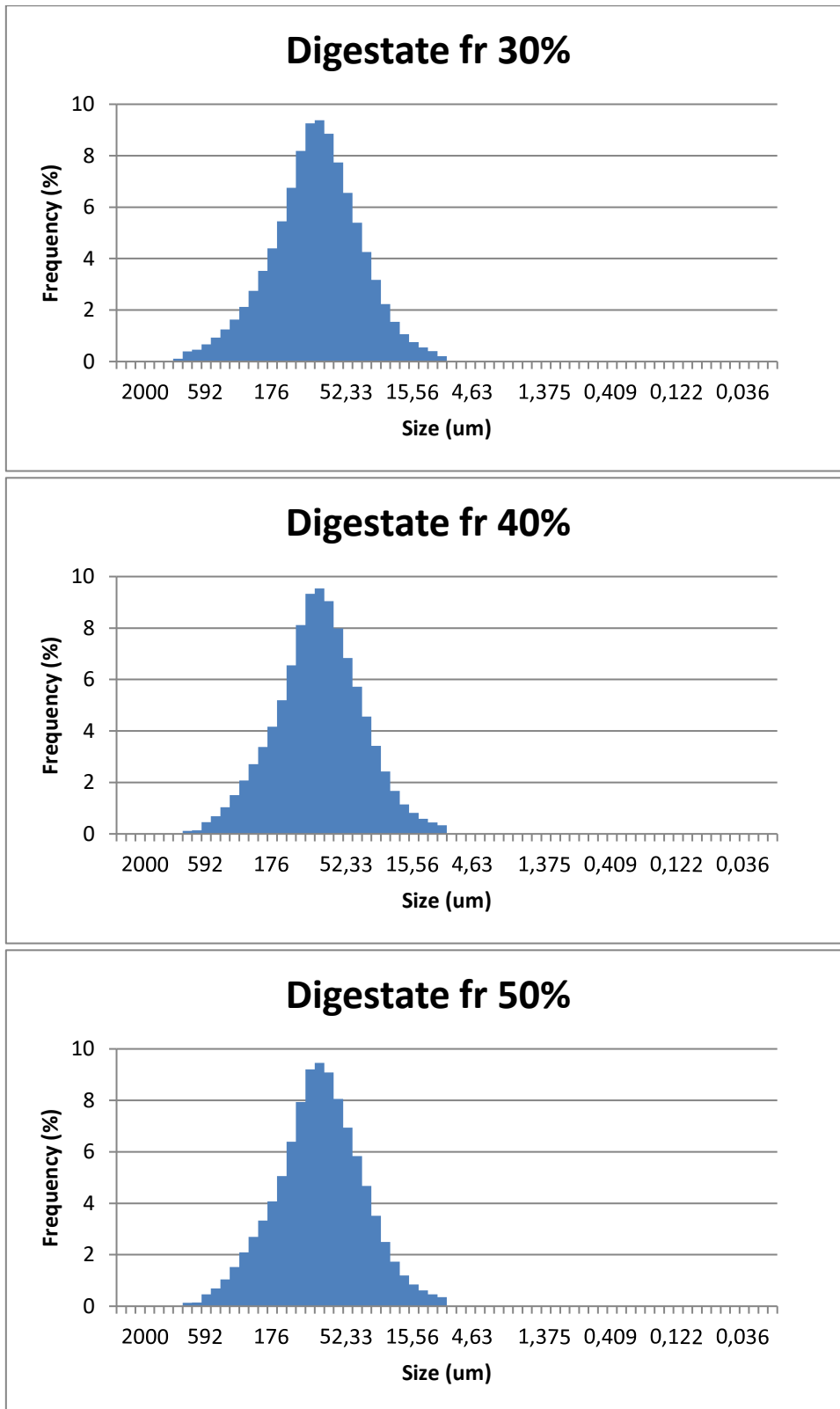
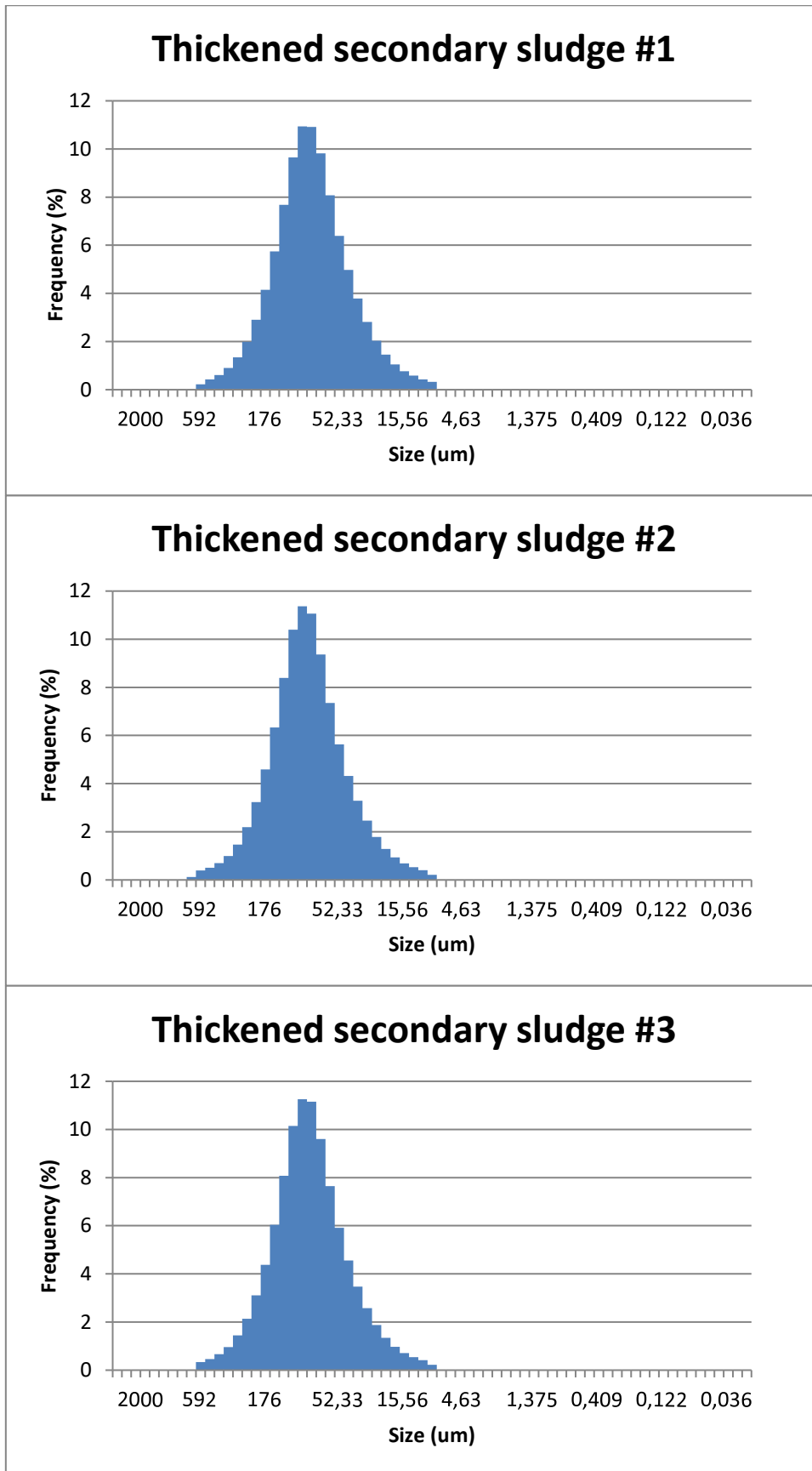**Figure C.2: PSD of digested sludge for 3 different flow rates (fr)**

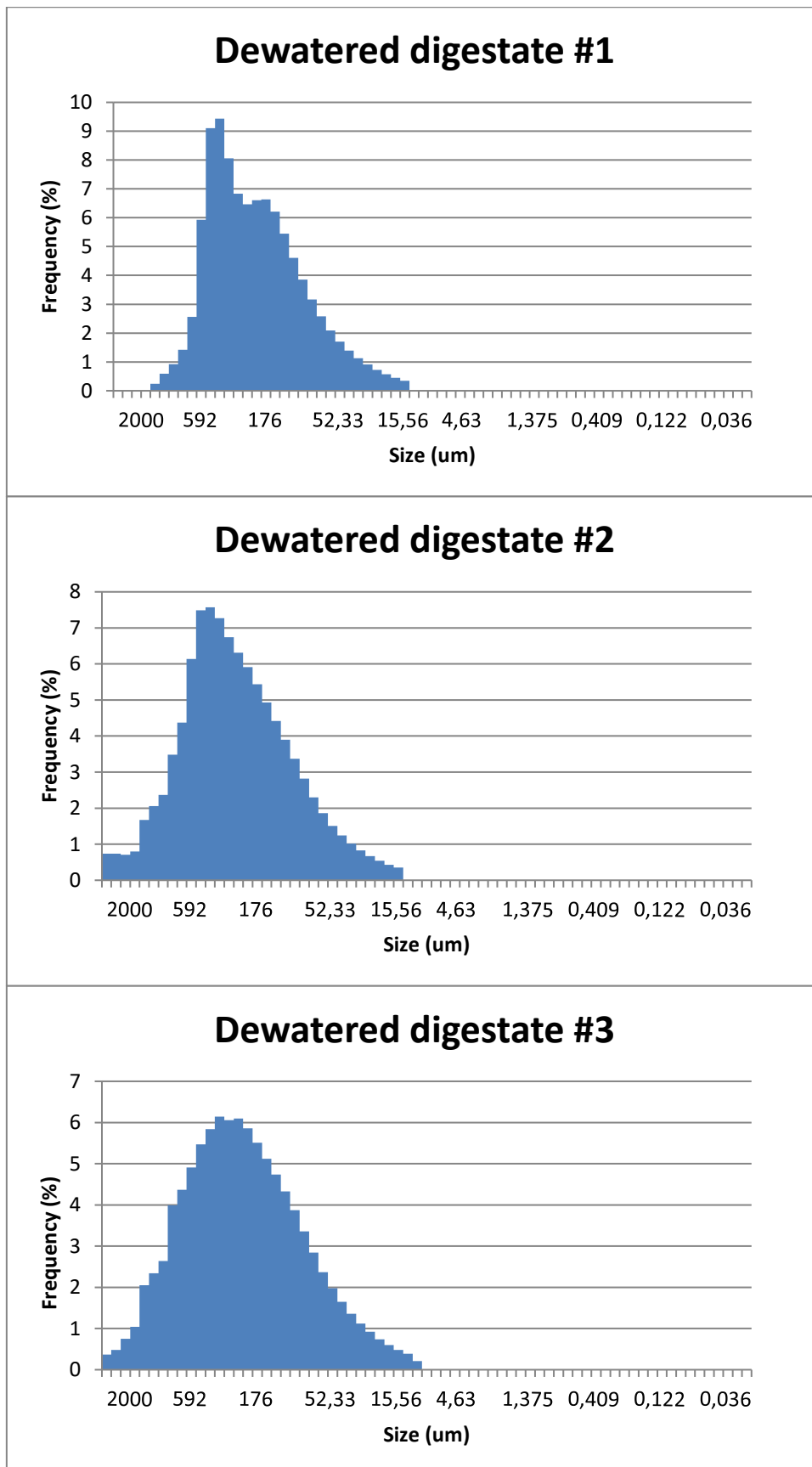**Figure C.3: PSD of thickened secondary sludge for 3 different samples of same batch at flow rate of 50%**

Figure C.4: PSD of digested sludge with DM of 22.75 wt% for 3 different samples of same batch at flow rate of 50%
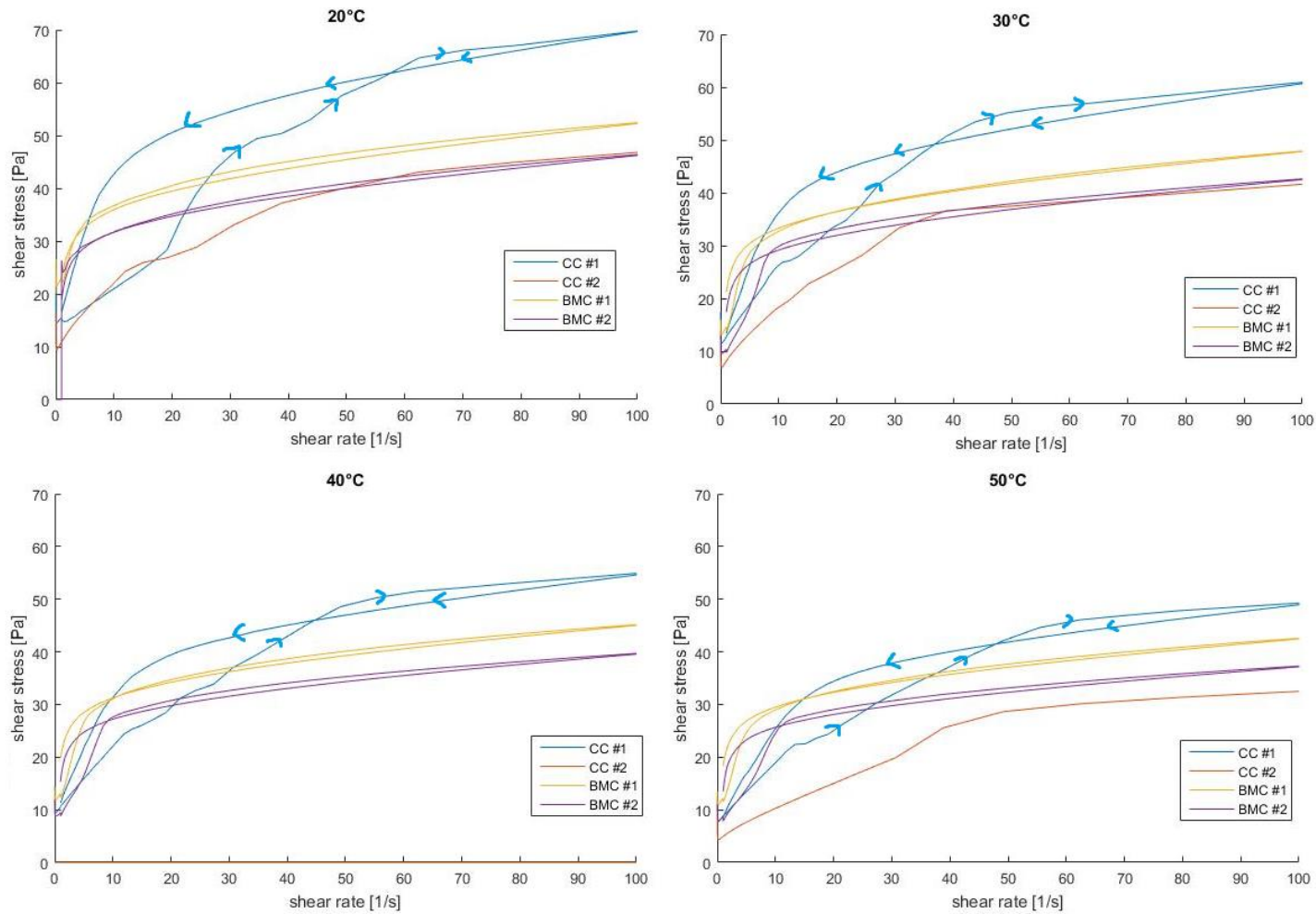
D   Results CC versus BMC

Figure D.1 Shear rate versus shear stress for thickened secondary sludge, both CC and BMC were tested with two samples, all four samples were collected on different dates, thus may vary in DM content

E   Results DM content with viscosity
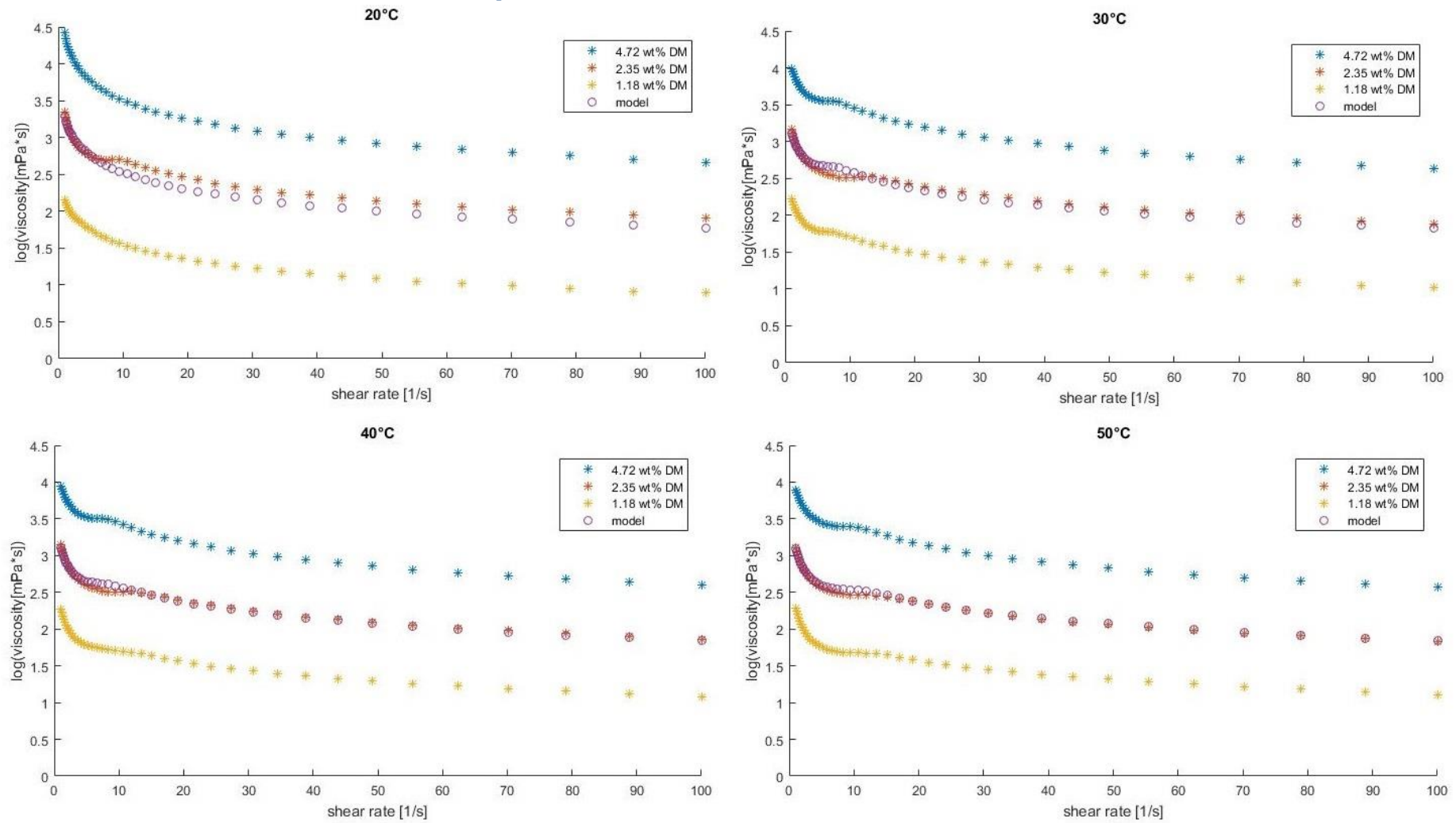
Figure E.1 Shear rate versus the log of the viscosity for different DM contents and model which describes the logarithmic correlation between DM and viscosity

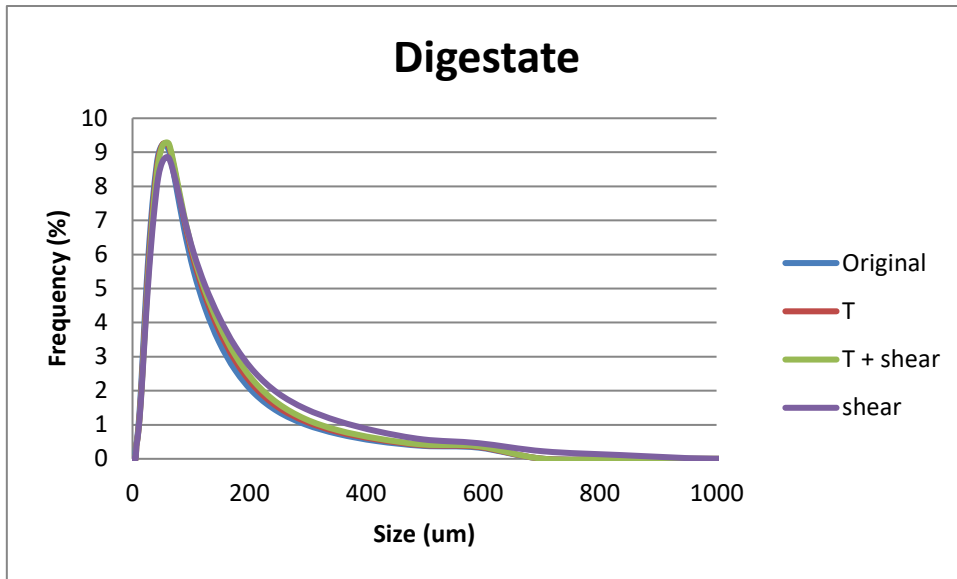# F   Results structural change upon temperature and shear
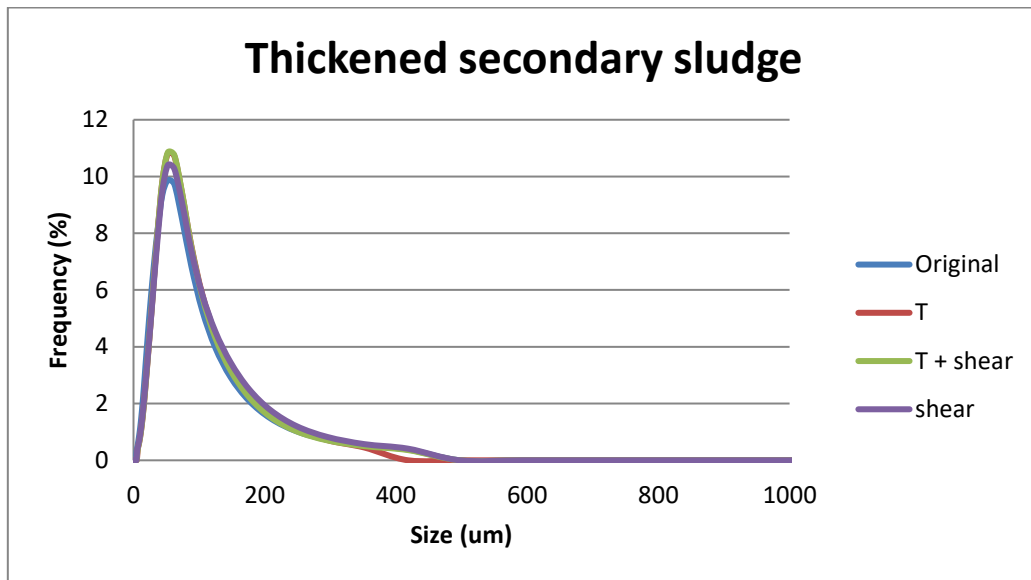
Figure F.1: PSD of thickened sludge for different pre-treatments conditions: no pre-treatment, high temperature, combination of high temperature & shear and shear only
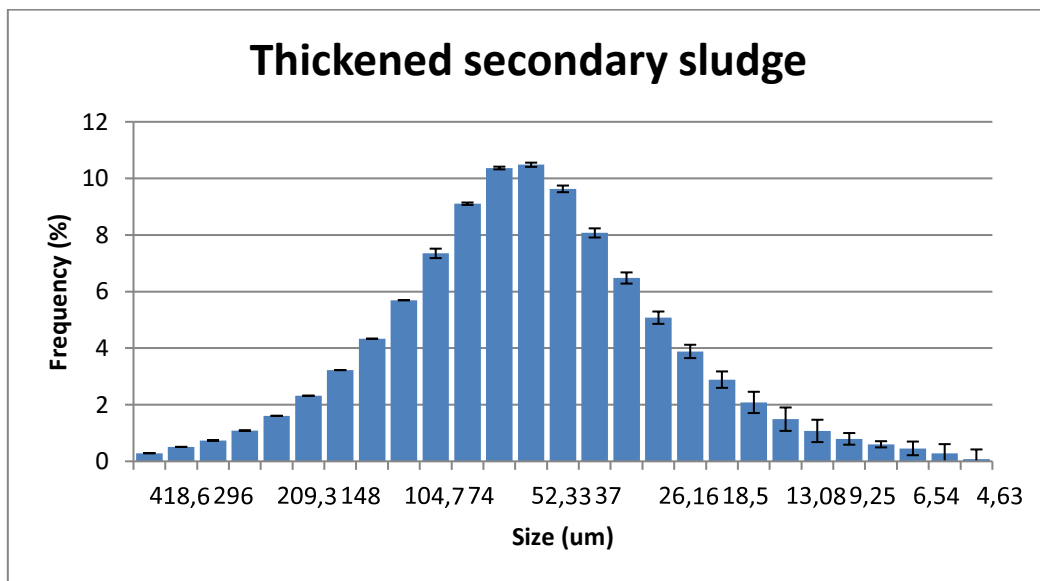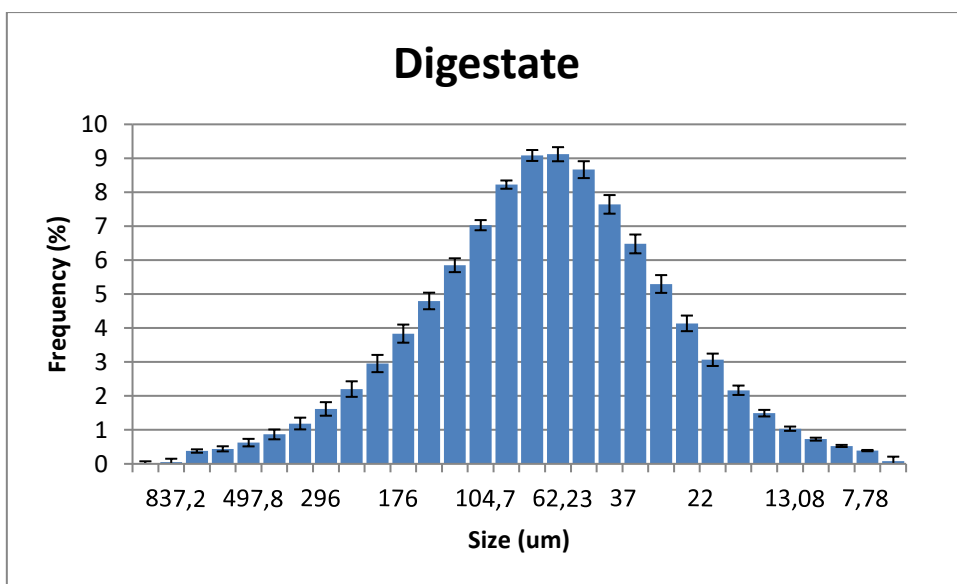

Figure F.2: Plot of average values from PSD of thickened sludge at all 4 conditions together including standard deviation bars

Figure F.3: PSD of digestate for different pre-treatments conditions: no pre-treatment, high temperature, combination of high temperature & shear and shear only

Figure F.4: Plot of average values from PSD of digestate at all 4 conditions together including standard deviation bars
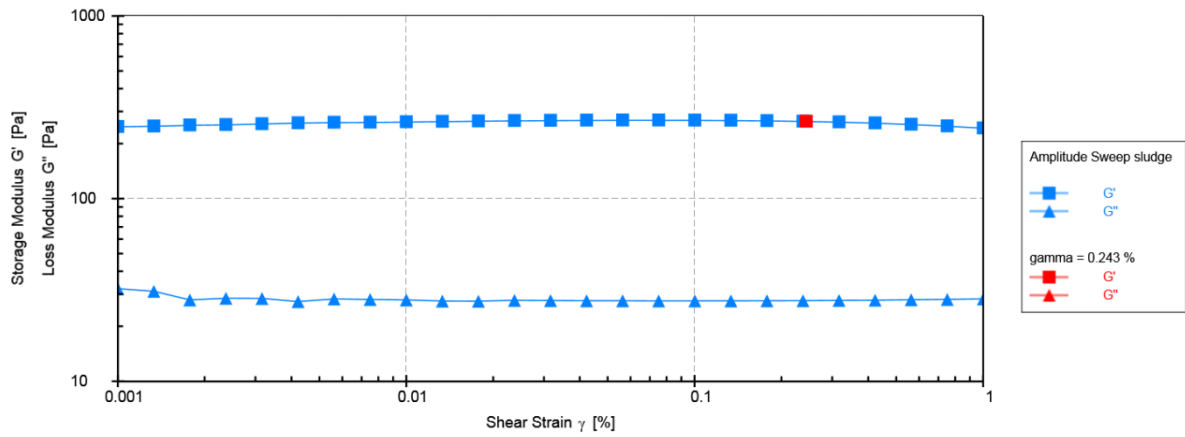
G Results amplitude sweep and frequency sweep

Figure G.1: Result of amplitude sweep test sludge, the red square indicates the limit value of the LVER
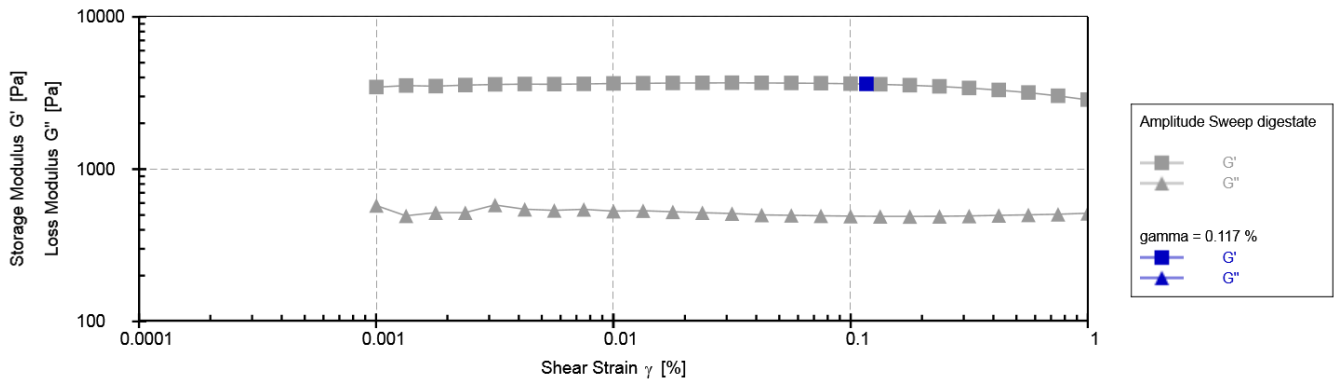

Figure G.2: Result of amplitude sweep test digestate, the dark blue square indicates the limit value of the LVER
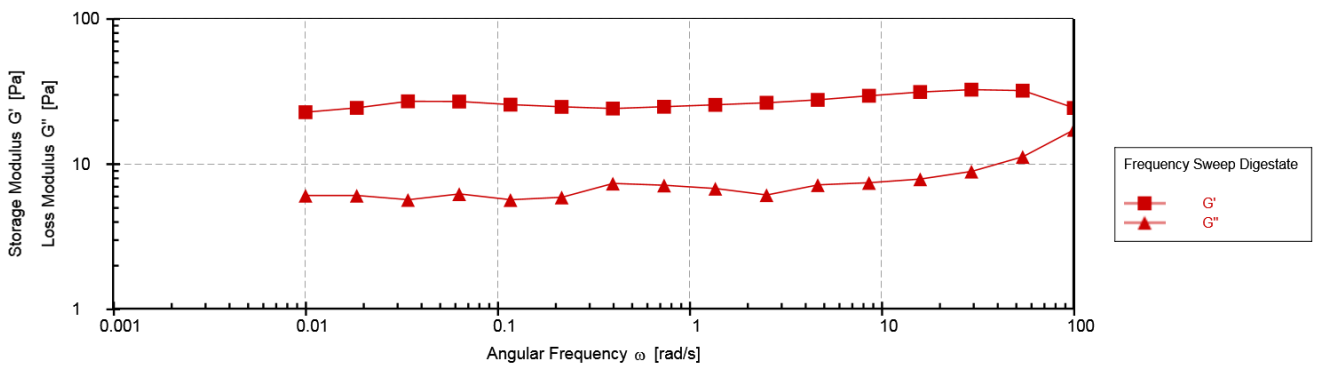

Figure G.3: Result of the frequency sweep test digestate, the square at 0.01 rad/s was used to determine the stability
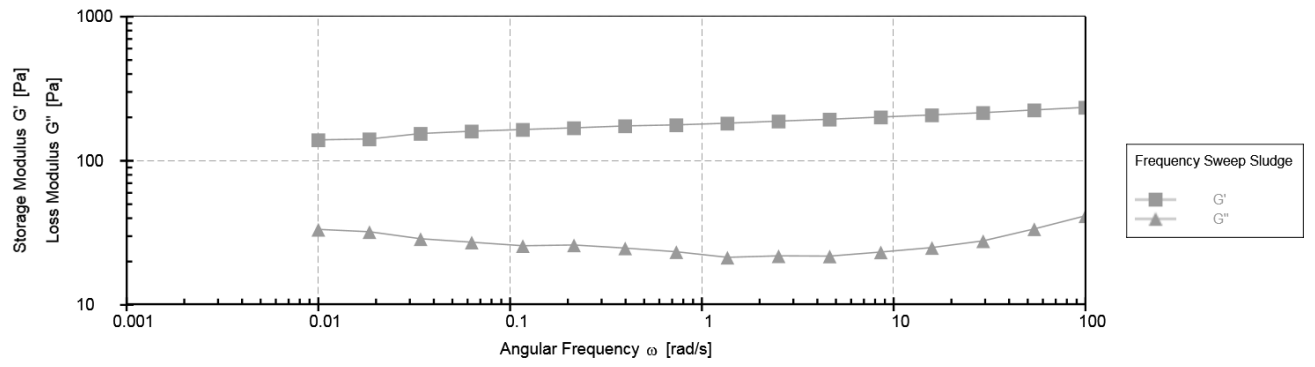
Figure G.4: Result of the frequency sweep test sludge, the square at 0.01 rad/s was used to determine the stability

H   MATLAB code for parameter estimation

```matlab
% Rheology of digestate presented in Ostwald- De Waele model (Power Law)
%       Estimate model parameters K and n which are dependent of
%       temperature
%       y = K*t.^(n);
%       With, n<1 for Pseudoplastic, n=1 for Newtonian fluid, n>1 for
%       Dilatant
% Programmer: Joanne Siccama

clear; clc; close all
format compact

%% load data
load digestate.mat
t = digestate(:,1);         % t is shear rate (1/s)

y1 = digestate(:,2);        % 20˚C
y2 = digestate(:,3);        % 25˚C
y3 = digestate(:,4);        % 30˚C
y4 = digestate(:,5);        % 40˚C
y5 = digestate(:,6);        % 50˚C

Y =[y1 y2 y3 y4 y5];                    % Y is shear stress (Pa)

T = [293;298;303;313;323];              % T is temperature (K)

N = length(Y);
nT = length(T);



%% fit parameters K and n on all data sets at once - K and n T dependent

tt = t*ones(1,nT);    % 40*5
TT = ones(N,1)*T';    % 40*5
XX = ones(N,1)*X;     % 40*5

for i = 1:nT;
   % find initial values
   % y = K/T*t^(n/T)
   % log(y) = log(K/T*tau^n) = log(K/T) + n*log(t)

   par_poly = polyfit(log10(t),log10(Y(:,i)),1);
   K = T(i)*10^par_poly(1)
   n = par_poly(2)/T(i)
   par0 = [K n];

end

% fit
F = @(par,tt)par(1)./TT.*tt.^(par(2)./TT);
[par,resnorm,~,exitflag,output] = lsqcurvefit(F,par0,tt,Y);
Yfit = F(par,tt);
err = sum(((Yfit(:,i) - Y(:,i)).^2./Y(:,i).^2))/N

K = par(1);
n = par(2);

% plot
```

```matlab
figure(i+1)
c = 'kbmrc';
for i=1:nT
    plot(0,0,'w.', t,Yfit(:,i),[c(i),'-'], t,Y(:,i),[c(i),'h'])
    hold on
end
title('Model with K and n are T dependent')
legend(['K=',num2str(K,'%0.1f'),',
n=',num2str(n,'%0.3f')],'fit','data','Location','southeast');
xlabel('shear rate [1/s]')
ylabel('shear stress [Pa]')
ylim([0 inf])
shg
```